

AD-A041 962

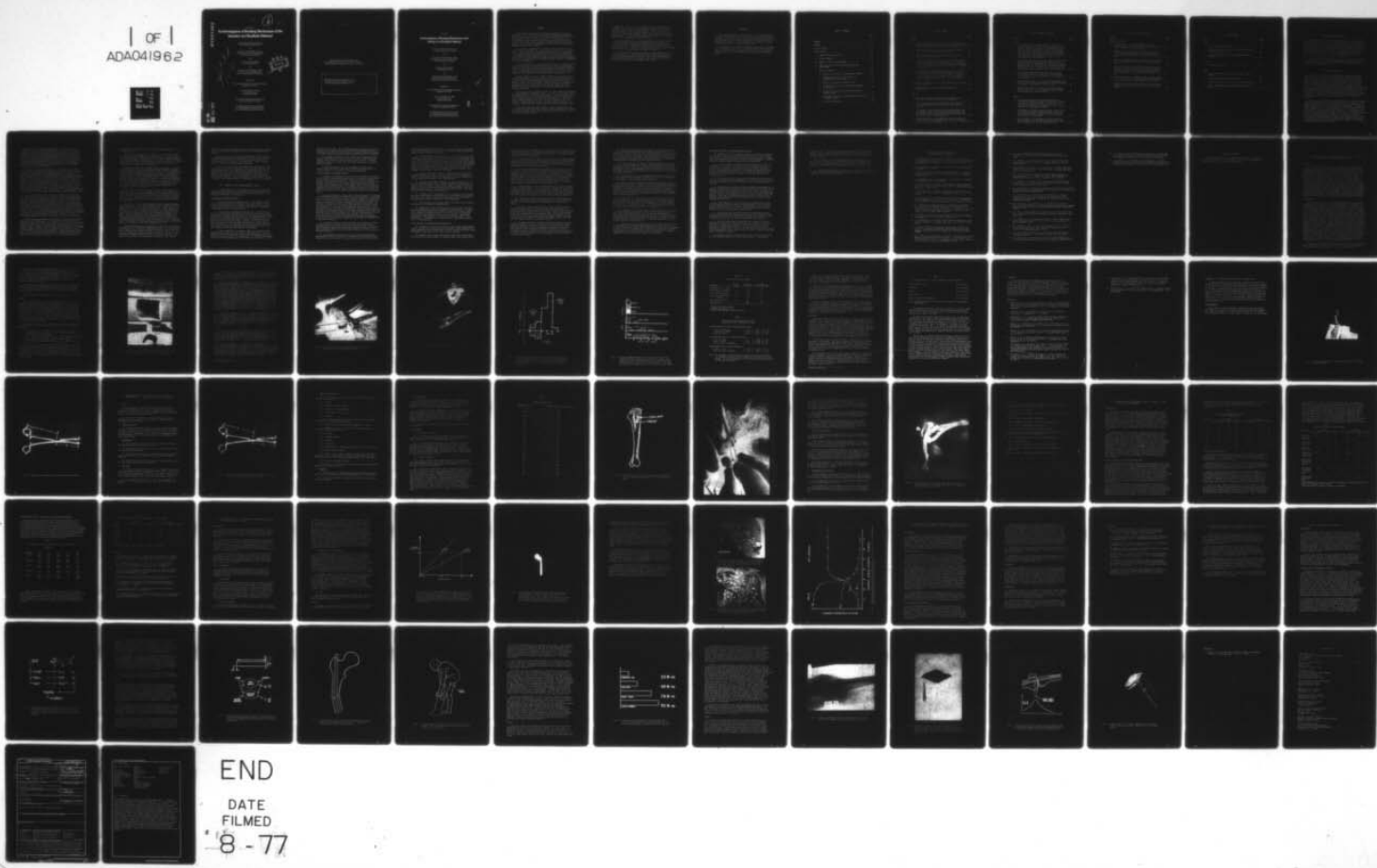
FLORIDA UNIV GAINESVILLE DEPT OF MATERIALS SCIENCE --ETC F/G 6/5
AN INVESTIGATION OF BONDING MECHANISMS AT THE INTERFACE OF A PR--ETC(U)
OCT 76 L L HENCH, W C ALLEN, H A PASCHALL

DAMD17-76-C-6033

NL

UNCLASSIFIED

| OF |
ADA041962



END

DATE
FILMED

8 - 77

ADA 041962

Report No. 7

— (6) 2

An Investigation of Bonding Mechanisms of the Interface of a Prosthetic Material

L.L. Hench, Department of Materials Science
and Engineering, University of Florida

and

H.A. Paschall, College of Medicine, J. Hillis
Miller Health Center, and Chief of Orthopaedics
Veterans Administration Hospital

and

W.C. Allen, College of Medicine
J. Hillis Miller Health Center

and

G. Piotrowski, College of Medicine, J. Hillis
Miller Health Center, and Department of
Mechanical Engineering, University of Florida



Supported by

U.S. Army Medical Research and Development Command
Washington, D.C. 20314

Contract No. DAMD 17-76-C-6033
University of Florida
Gainesville, Florida 32611

This document has been approved for public release
and sale: its distribution is unlimited

The findings in this report are not to be construed
as an official Department of the Army position
unless so designated by other authorized documents.

NO. _____
DOC FILE COPY

()

Qualified requestors may obtain additional copies
from the Defense Documentation Center. All others should apply
to the Clearinghouse for Federal Scientific and technical Information.

This public document was promulgated at a cost of
\$935.00 or \$1.87 per copy to provide an annual report
to the supporting group of this ongoing research.

AD_____

Report No. 7

An Investigation of Bonding Mechanisms of the Interface of a Prosthetic Material

L.L. Hench, Department of Materials Science
and Engineering, University of Florida

and

H.A. Paschall, College of Medicine, J. Hillis
Miller Health Center, and Chief of Orthopaedics
Veterans Administration Hospital

and

W.C. Allen, College of Medicine
J. Hillis Miller Health Center

and

G. Piotrowski, College of Medicine, J. Hillis
Miller Health Center, and Department of
Mechanical Engineering, University of Florida

Supported by

U.S. Army Medical Research and Development Command
Washington, D.C. 20314

Contract No. DAMD 17-76-C-6033
University of Florida
Gainesville, Florida 32611

This document has been approved for public release
and sale: its distribution is unlimited

The findings in this report are not to be construed
as an official Department of the Army position
unless so designated by other authorized documents.



SUMMARY

This research program has had two primary objectives since its inception: (1) to achieve a direct chemical bond between orthopaedic devices and bone using surface active glass and glass-ceramic materials or coatings, and (2) to develop a scientific understanding of the chemical and mechanical interfacial reactions occurring between materials and bone. This report summarizes progress toward realizing these objectives by reviewing accomplishments of the past six years and presenting a series of new findings.

The influence of phosphorus, boron and fluorine additions on the surface chemical reactivity of a soda-lime-silica glass has been investigated. Several techniques, including infrared reflection spectroscopy, ion solution analysis, scanning electron microscopy, energy dispersive x-ray analysis, x-ray diffraction, Auger electron spectroscopy and ion beam milling, have been employed to develop insight into the morphological and chemical changes which occur in glass surfaces corroded in a simulated physiologic environment.

The resulting corrosion layers and the influence of phosphorus, boron and fluorine on their compositions and rates of formation are defined. Surface ion concentration profiles determined with Auger spectroscopy and ion beam milling detail the structural alterations produced by aqueous attack. A mechanism is postulated which explains the sequence of events leading to the formation of the multiple-layer corrosion structures.

Having defined the surface chemical behavior of the glasses in an in vitro environment, an effort is made to relate these observations to the response elicited when identical glasses are implanted in laboratory animals. Stable interfacial fixation results when specific surface chemistry conditions are satisfied. Some of the events postulated by the in vitro studies as initial steps in the bonding process have been identified in samples implanted for one hour and examined with Auger electron microscopy.

The in vivo results demonstrated that the four compositions implanted all exhibited direct attachment to bone. There was a wide variation in the appearance of the tissue near the implant. Only the interface of the glass containing 6 wt. % P₂O₅ exhibited a healthy zone of ossification characterized by numerous osteocytes in close proximity to the glass, a layer of unmineralized osteoid, and a layer of osteoblasts actively engaged in laying down new osteoid. The other glasses exhibited a low density of viable osteocytes and an absence of an active osteoid front.

Based upon the in vivo observations, a theory is proposed that an ideal implant material must have a dynamic surface chemistry that induces histological changes at the implant surface which would normally occur if the implant were not present.

Mechanical tests of bones containing segmental replacements of bioglass-ceramic showed that the structural strength of the implanted bone was about 75% that of the intact bone. Analysis of the fracture site by the SCADS computer program showed that the interface is at least as strong as the bioglass-ceramic, and at least 75% as strong as the host bone. Fractures occurred through the implant or through the bone, but not preferentially at the interface.

An in vivo proof test of the bonding ability of bioglass formulations in rat tibiae has been developed and implemented. This test isolates the material-dependent determinants of bond formation from other factors, such as geometrical and mechanical factors. This test has also been used to demonstrate that replacement of sodium by potassium does not affect the formation of the bioglass-bone bond.

A material system involving a bioglass coating on stainless steel holds much promise for combining the strength of the metal substrate with the bone-bonding surface bioglass. The process is applicable to a wide variety of metallic devices and forms a very stable interface, which is not preferentially attacked by body fluids.

FOREWORD

The program undertaken in the contract is an interdisciplinary effort of the Departments of Materials Science and Engineering and Mechanical Engineering, College of Engineering, University of Florida; the Departments of Orthopaedics and Anatomy, College of Medicine, University of Florida; and the Department of Orthopaedics, Veterans Administration Hospital, Gainesville, Florida.

In conducting the research described in this report, the investigators adhered to the "Guide for Laboratory Animal Facilities and Care," as promulgated by the Committee on the Guide for Laboratory Animal Resources, National Academy of Sciences-National Research Council.

TABLE OF CONTENTS

	Page
SUMMARY	2
FOREWORD	4
LIST OF FIGURES	6
LIST OF TABLES	9
I. INTRODUCTION AND OBJECTIVES	10
II. PROJECT OVERVIEW	10
III. SUMMARY OF MAJOR ACCOMPLISHMENTS	13
IV. CUMULATIVE LIST OF PUBLICATIONS RESULTING FROM THE CONTRACT	20
V. REVIEW OF PROGRESS	23
A. Mechanical Evaluation of Bone-Bioglass Bonding	24
B. Standard Method of Test for Ability of a Biomaterial to Bond to Bone	40
C. Material Screening for Bonding Ability	50
D. An Immersion Process for Coating Metal Implants With Bioglass	55
E. Studies in Artificial Bone Graft Materials--A Progress Report	62
F. Histological Studies of the Bone-Bioglass Interface-- A Progress Report	65
G. Clinical Biomechanics	66

LIST OF FIGURES

Figure	Page
<u>Part A</u>	
1. Excised femur from canine push-out study with soft tissue removed (A), transversely sectioned into individual coupons (B), and machined and placed in the test fixture (C)	26
2. Implantation of test coupon into the anterior border of the rat tibia for the mini-push-out test	28
3. Excised rat tibia, soft tissue removed, placed in the mini-push-out loading forceps	29
4. Torsional strength data for primate model illustrating the fracture strength of the control group (A), the strength of the osteosyntheses which fractured away from the implant (B) and the calculated interfacial stresses at the implant at fracture (C)	30
5. Histogram summarizing the forces to push out the various compositions tested using the canine model. Except for the bioglass specimens, one specimen from each group was tested at 28 days due to fracture of one of the femurs. All of the bioglass specimens were tested at 28 days for the same reason	31
6. Ratchet configuration of the sponge forceps in the zeroing (first) position	38
7. Sponge forceps showing the lengths used during calibration	39
<u>Part B</u>	
1. This modified sponge forcep is used to apply the push-out force to the test specimen after sacrifice	41
2. The location of the implant immediately post-operatively should be immediately posterior to the tibial crest, as shown	45
3. The implant is being inserted in the defect machined into the proximal tibia. The periosteal elevator shown in the background is used to maintain the musculature around the tibia away from the implantation site	46
4. The adjusting screw of the modified forcep is adjusted to contact one end of the implant, while the bone is supported by the other jaw of the forcep	48

LIST OF FIGURES (Continued)

Figure	Page
<u>Part D</u>	
1. The coefficient of thermal expansion of the metal, α_m , is larger than that of glass, α_g , but just prior to immersion the metal is heated to a temperature T_m such that the actual expansions of the metal and the glass are equal at E_p . The immersion time is short enough that the metal doesn't have time to heat up and expand. After immersion, both materials cool down to room temperature and contract equally	57
2. This femoral head prosthesis for a monkey was fabricated by the College of Engineering Shop coated with the immersion process. Total length of the device is approximately 65 mm. The coating on the stem was machined by grinding to produce a uniform cross section, while the glass coating of the head was left in its natural form . . .	58
3a. This SEM micrograph illustrates the cross section of the interface produced by immersing a 316L stainless steel piece (M) into 45S5 bioglass (G). The white bar is 50 μm long	60
3b. The fracture surface of 45S5 bioglass flame-sprayed onto stainless steel shows many voids, some of which penetrate to the metal. The white bar is 50 μm long	60
4. Compositional analysis across the interface shown in Figure 3a shows a 2 μm wide transition region between the stainless steel and the bioglass	61
<u>Part G</u>	
1. All biomechanical analysis approaches make use of equilibrium conditions, geometric compatibility, and/or constitutive relations to deal with the object of interest, as defined by the "free body," and to attain solutions to biomechanical problems	67
2. The analysis of stresses and deflections requires that the loading, obtained as shown in Figure 1, and the material properties be combined with the description of the object's configuration	69
3. This tracing of an X-ray shows the bend suffered by a 9 mm cloverleaf nail when the patient puts on his pants while standing up at 3 weeks post-operatively	70

LIST OF FIGURES (Continued)

Figure	Page
<u>Part G</u> (continued)	
4. Configuration of a subject filmed in the act of dressing himself. Note the position of the upper body is far in front of the fracture site	71
5. Comparison of the strengths of the cloverleaf nail, a solid rod of stainless steel, an intact femur, and the bending moment applied to the thigh at the fracture site	73
6. X-ray of a Hansen-Street nail, intended to fuse the knee, which failed abruptly about three years after implantation	75
7. The fracture surface of the implant shown in Figure 6 presents an appearance typical of a fatigue in reversed bending. The central ridge running horizontally across the diamond-shaped cross section was the last part to fail	76
8. Freebody analysis of the implant shown in Figure 6 prior to its failure shows that the bending moment experienced by the nail is quite constant across the joint space	77
9. Another view of the fracture surface of the nail shows another fatigue crack about 5 mm distal to the fracture surface	78

LIST OF TABLES

Table	Page
<u>Part A</u>	
1. Canine Push-Out Data Summary	32
2. Statistical Results (Student's t Test) Determined for the Canine Push-Out Data	32
3. Arithmetic Average of Surface Roughness of Canine Implants	34
<u>Part B</u>	
1. Nembutal Dosage Chart	44
<u>Part C</u>	
1. Results of Mini-Push Out Test for 10 Lots of 45S5 Bioglass	51
2. Summary of Material Screening Studies	52
3. Compositions Used to Study Effect of Na-K Substitution . .	53
4. Effect on Bonding Ability of Substitution of K ₂ O for Na ₂ O	54

I. INTRODUCTION AND OBJECTIVES

There are two primary objectives in this program. 1) To achieve a direct chemical bond between a ceramic material and bone. Accomplishment of this objective will enable the development of a wide range of orthopaedic prosthetic devices which will not loose with time and require removal from the patient; and 2) to develop a scientific understanding of the chemical, biological and mechanical interfacial reactions occurring between materials and bone. Accomplishment of this objective will enable the engineer and physician to collaboratively design a materials system to satisfy a specific combination of mechanical and physiological requirements in medical applications.

Previous progress in achieving these objectives has been discussed in Reports No. 1, 2, 3, 4, 5 and 6 prepared for this contract in August 1970, August 1971, August 1972, September 1973, September 1974, and September 1975, respectively.

II. PROJECT OVERVIEW

In order to meet the above objectives, glass and glass-ceramic materials have been developed which promote the formation of a direct chemical bond at the interface of the material and bone. The direct bond is obtained without the use of a porous structure in the glass-ceramics, thereby retaining the intrinsic strength of these materials and also enabling the glass-ceramics to be used as coatings on high strength metal or other ceramic substrates. As discussed in Reports No. 1, 2, 3, 4, 5 and 6, promotion of the chemical bonding is accomplished by incorporating into the glass-ceramic structures soluble sodium, calcium and phosphate ions in ratios which can influence the precipitation of hydroxyapatite in bone. Variable rates of ion release have been achieved by varying (1) and Ca/P ratio, (2) the percentage of network formers in the glass, (3) the type of network former (SiO_2 or B_2O_3), and (4) F^- additions.

Previous in vitro studies have been conducted to establish parameters controlling the bonding of the glass-ceramic materials with bone. These studies have demonstrated that the phosphate containing glass-ceramic surface enhances surface crystallization of hydroxyapatite. Studies presented in Report No. 4 showed what appeared to be a hydroxyapatite-like layer forming on top of a silica-rich layer, due to the reaction of bio-glass with an aqueous medium in vitro. The role of a soluble SiO_2 gel layer at the implant interface appears to be critical for bonding in light of recent studies showing SiO_2 present as an osteogenic precursor. Certain protein macromolecules also bond to the bioglass-ceramic surface in a dense, randomly distributed conformation in contrast to a highly oriented distribution on quartz surfaces and a complete lack of bonding on other mineral and ceramic surfaces.

The degree of selective attack of the silicate network and the resulting corrosion layers are influenced by the quantity of phosphate in the glass, with the addition of phosphate producing a double layered corrosion film which is more effective in protecting the bulk glass from aqueous attack. Detailed concentration profiles of corroded bioglass surfaces have been obtained with Auger Electron Spectroscopy and ion beam milling which confirm the existence of the silica-rich gel and a very thin calcium phosphate film at the surface. The crystalline product which grows from the initially amorphous calcium phosphate film has been identified as hydroxyapatite which contains a considerable quantity of CO₂ within its structure.

Implantation of duplicate bioglass-ceramic samples in rat femurs has been used to evaluate the formation of the chemical bond at a living interface. Tetracycline tracers, microradiography, scanning electron microscopy, light microscopy and transmission electron microscopy all show evidence of new bone growth contiguous with the bioglass and bioglass-ceramic implant surface. A viable bond forms as early as 10 days post-operatively. A histological sequence shows that mature bone appears at points on the active glass-ceramic surface at four weeks. After twelve weeks a complete mature laminar interface has been established. Transmission electron micrographs show an amorphous gel-like layer immediately adjacent to the implant surface, with highly elongated hydroxyapatite crystals bridging the gap between the implant and the mature bone which has formed around the implant. These hydroxyapatite crystals apparently form after osteoblasts have laid down collagen fibers on this silica gel layer.

In vivo studies presented in Report No. 5 support the contention that a silica-rich gel on the glass surface serves as the induction site for ossification. Four bioglasses, including a soda-lime-silica glass and three compositions produced by adding 3, 6 and 12 wt. % P₂O₅ to the ternary glass, exhibited direct attachment to bone at three weeks. As the ternary glass only forms a silica-rich surface, even when phosphates are present in solution, and the glass-bone interface appears very similar for all four compositions, it seems likely that the silica-rich layer is serving as the site for osteoblasts to lay down the organic intercellular substance of bone. The calcium phosphate layer which develops a phosphorus is added to the bioglass composition and may serve as a source of ions to be incorporated into the mineralization process. However, an excess of calcium and phosphate ions lead to cell death and ectopic calcification.

Bioglass specimens implanted in rat femurs for one hour were examined using Auger electron microscopy and ion milling techniques in order to study compositional variations at the implant surface. As with the samples corroded in vitro, the silica-rich gel was found, covered by a calcium phosphate layer. However, a very important difference was that the in vivo reactive surface contained organic constituents to a depth of 180 nm. The calcium phosphate film in the in vivo sample was also thinner, placing the silica-rich layer closer to the surface. Transmission electron microscopy of the bioglass-bone junction shows ultrastructural evidence of the same sequence of chemical constituents. It is the "graded interface"

that apparently is responsible for the high mechanical strength of the bioglass-bone bond.

The mechanical strength of the interfacial bond developed between a glass-ceramic bone implant with a reactive surface and a rat femur was measured. After 28 weeks sufficient strength was established that the bone failed under a torsional stress of 50 mPa (513 kg/cm^2) with the glass-ceramic interface remaining intact. Computer programs to evaluate stresses actually applied at the implant interface are used in the interpretation of the mechanical test data.

Statistical evaluation of segmental femur replacements in monkeys showed development of a strong interfacial bond. Torsional strength of the bone implant system was measured to be about 75% of the strength of the intact femur. Fractures were observed in either the bioglass-ceramic or in the bone, but did not preferentially propagate along the bone-implant interface. Since the interfaces were not fractured during the torsional tests, the strength of the interface could not be determined, but lower limits could be assigned. Analysis of the fracture and interfacial shear stresses showed that the interface sustained stresses of over 78 MPa (800 kg/cm^2), which is about 75% of the strength of the healing bone. This strength level also represents about half the strength of normal cortical bone.

Partial hip prostheses for stumptail monkeys were designed using biomechanics factors. The 316L surgical stainless steel prostheses flame spray coated with bioglass showed stable fixation in the medullary canal without the use of screws or other mechanical means of fixation. Functional use of the hip was retained. Histological evaluation after one year showed complete protection of neighboring tissues from metal corrosion products.

An effort to utilize sintered alumina-bioglass composite materials as resorbable bone plates for the fixation of fractured bones led to a program to optimize the strength of the material. A bone plate was designed for the fixation of transverse fractures of canine femurs and six implantations were performed. While most plates failed within 10 days, one plate survived until the bone healed and was removed at 64 weeks. The plate showed no evidence of resorption or bonding to the bone. In fact the underlying bone showed radiological evidence of resorption away from the plate. Some tissue necrosis in the vicinity of sintered materials implanted in rat tibias was also noted, suggesting that for bioglasses to be effective they must be presented as an as-cast glass or as a glassy coating with minimal microporosity.

A rapid and inexpensive technique has been developed for assessing the bonding ability of bioglass formulations *in vivo*, and has been used to demonstrate that bonding is attained consistently with the 45S5 bioglass. The same test is now being used as a quality control test for all other implantation studies, thereby assuring that materials used for biomechanical studies have the ability to form bonds with bone. The effect of variations in the composition of bioglass on the bonding

ability is also being scrutinized, and it has been found that substitution of potassium for sodium does not affect the bonding ability of bioglass.

A new process for coating metallic implants with bioglass using an immersion technique has been developed. The metal-glass interface formed is quite resistant to attack by body fluids, and the metal-glass transition is only about two microns thick. Thus, a bioglass surface is presented to the in vivo environment.

A series of canine fibular replacements have demonstrated a uniform lack of bond formation, despite the fact that the materials used had previously passed the in vivo test for bonding ability. Lack of fixation appears to be the prime interference to bond formation. The implants were encapsulated in callus within only a few weeks, and motion of the implant was thereby eliminated, but the bond did not form at this later time. Thus the mechanism of bond formation appears to involve a time sequence which, if interrupted, will not be completed.

III. SUMMARY OF MAJOR ACCOMPLISHMENTS, 1969-76

1. A systems analysis of the various activities in the research program has been completed and has been used to establish budget and personnel allocations as well as the time sequencing required for the interacting functions of the research.

Development of Materials Systems

2. The basic bioglass composition, 45S5, is an invert soda-lime glass, containing 45% SiO₂ as network former, equal amounts (24.5%) of Na₂O and CaO, and 6% P₂O₅, by weight. This material can be used in its as-cast (glassy) form, or partially crystallized, or completely crystallized to become a bioglass-ceramic.

3. Low viscosity, biocompatible glasses with a variable rate of release of surface ions and changes of surface pH have been developed. This series of glasses, 45B₁₅S5 and 45B₅S5, involved the partial replacement of the SiO₂ network forming oxide with B₂O₃ network formers. The Na₂O-B₂O₃ ions in the glass complex to form a tetrahedral structural unit akin to that of the SiO₂ units. However, the viscosity of the glass is greatly reduced, thus making it possible to flame spray or enamel the bioglass. Both in vitro and in vivo evaluations establish the equivalent behavior of this new line of bioglasses to that of the 45S5 composition originally developed in this program.

4. A third composition of bioglass, 45S5F, was developed by substituting CaF for about half of the CaO. These glasses show similar behavior to the other bioglasses, both in vivo and in vitro, and lower viscosity than the original 45S5 composition. The 45S5F glasses evolved for use in a flame-spraying process developed in collaboration with the

ceramics group at IITRI. The flame-spraying process was used to successfully coat such complex devices as femoral head replacement prostheses for monkeys completely with 45S5 bioglass, thereby combining the strength of the metal with the desirable surface characteristics of the bioglass.

5. An immersion process for coating metal with bioglass has been developed and shown to produce surfaces equivalent to bulk bioglass in terms of tissue response. With this process the strength of the metal substrate can now be combined with the surface properties of bioglass within an implant.

6. Other material systems, such as enameled stainless steel sintered bioglass-ceramics, and bioglass-alumina composites, have been tested and found to be unsuitable for in vivo implantation.

In Vitro Studies of Bioglass Surfaces

7. Methods for evaluating the specific ions released at the surface of the bioglasses and bioglass-ceramics and the structural changes in the implant surfaces have been developed. These include atomic absorption analysis, atomic emission analysis, colorimetry, infrared reflection spectroscopy, scanning electron microscopy. Auger spectroscopy has been recently used to understand the exact chemical nature of the interfacial surface of the implant materials. Ion-milling of the surface followed by segmental Auger spectroscopy reveals the detailed sequence of Na, Si, Ca and P ions released from the implant surface and build-up of surface gel layers.

8. In vitro evaluation of the surface chemical response of bioglasses to a simulated physiologic environment has been accomplished. A corrosion layer or layers is formed as a result of aqueous attack of the glass structure. If phosphorus is absent from the bioglass composition, sodium and calcium are selectively leached, producing a silica-rich gel layer. The addition of phosphorus to the glass composition does not interfere with the development of a silica-rich gel layer initially. However, a second film composed of an amorphous calcium phosphate develops at the silica gel-water interface and with time crystallizes to form an apatite structure. Increasing the phosphorus content of the glass composition accelerates the formation of the calcium phosphate film. Partial substitution of B_2O_3 for SiO_2 accelerates the initial dissolution process. The addition of fluorine to the glass composition significantly enhances the resistance of the glass to aqueous attack, probably by substituting for hydroxyl ions in the apatite structure.

9. Composition profiles of the corrosion layers formed on a series of bioglasses with increasing phosphorus content have been measured employing Auger Electron Spectroscopy and ion beam milling. The profiles provide detailed compositional maps which confirm the existence of the calcium phosphate gel-silica gel-bulk glass structure at the bioglass surface after reaction.

10. Conditioning of bioglass with tissue culture medium prior to implantation fosters the formation of an intimate and ultrathin calcium phosphate film on the implant. This prevents spalling of the film which

occurs with untreated implants because the calcium phosphate film forms very rapidly and becomes quite thick. As a result, conditioned implants appear to form a stronger bond to bone.

11. Long-term studies (>10,000 hours) of the solubility and pH-time dependence of the various bioglass and bioglass-ceramic compositions show a controlled release rate of Ca, Na, Si and P ions from the implant surfaces. The ion losses in buffered solutions provide the physical-chemical correlation required to interpret the soft tissue and hard tissue in vitro responses. Fluorine additions decrease the ion release rate and thereby evoke a slower mineralization. Boron oxide additions accelerate the interfacial reactions. Thus, the bioglass and bioglass-ceramics can be designed to match specific metabolic activities.

12. In vitro solubility studies on flame sprayed 45B₅S₅ and 45S₅F bioglass-ceramics, 45S₅ fusion coated on alumina, and 45S₅ immersion coated on 316 stainless steel, have shown that the relative solubilities of these materials is similar to the bulk materials.

13. In vitro studies have shown that the crystal structure of the glass-ceramic will promote direct chemical bonding of hydroxyapatite crystals at the interface. These results suggest a mechanistic explanation for the direct bonding achieved in the in vivo studies. They also suggest means of directly controlling bonding and interfacial reactions desired in specific medical applications.

14. Precipitation of polypeptides on the surfaces of glass-ceramics and various other minerals have shown that the compatibility of proteins is a function of crystal structure and orientation of the crystalline materials surface and is a function of glass composition.

15. The bioglasses and bioglass-ceramics developed in this program bond with certain charged polypeptide groups.

16. Application of the protein-mineral epitaxial results obtained in this program has been made to the problem of urolithiasis. The interfacial interactions between the inorganic substances and organic matrix in the formation of urinary stones is akin to the type of interfacial interactions being examined in detail in this contract. Consequently, application of these results to other medical problems appears to be possible and our research has provided guidance on these matters wherever it seems justified.

In Vivo Studies of Bioglass-Tissue Interactions

17. Techniques to evaluate the nature of interfacial bonding between ceramics and bone have been successfully developed. These techniques include transmission electron microscopy, scanning electron microscopy, micro-radiography, tetracycline tracers and optical microscopy.

18. Nonporous 45S₅ bioglass and bioglass-ceramic have been found to attach directly to bone by means of a chemical bond. The strength of the

bond is sufficient that implants in rat femurs cannot be forcibly extracted. The bonding strength is sufficient that the interfacial attachment of the ceramic to the bone will withstand the implant force of a milling machine cutting bar and diamond microtome.

19. Confirmation and extension of our earlier bone-bioglass-ceramics interface reaction mechanism studies have been achieved by comparing 45S5, 45B₅S5 and 45S5F bioglass-ceramics implanted in the cancellous bone of the proximal tibia of young rats. All of the implants grew with the newly forming bone away from the epiphyseal plate.

20. Ultrastructural studies of the bone-ceramic interface have led to a theory of the formation of the bond through the production of an amorphous ion surface gel on the bioglass. An amorphous gel-like layer has been noted on the surface of the implant, extending over a distance of 800 to 1,000 Å. This layer may be equivalent to the substance comprising the "cement line" in mature bone. Osteoblasts lay down collagen fibers onto this bonding layer and mineralization then occurs in an ectopic manner. The resulting, highly elongated, crystals bridge the space between the implant surface and the mature bone.

21. Implantation of a series of bioglasses with variable phosphorus content has given support to the concept of the soluble silica-rich gel serving as an induction site for osteogenesis. In addition, there is an optimum phosphorus level in the bulk composition which leads to a situation where a sufficient but not excessive supply of calcium and phosphate ions is available for incorporation into the mineralization process.

22. Partial or complete substitution of potassium for sodium does not impair the formation of the bone-bioglass bond. This suggest that the role of these two elements in the formation of the bond is very similar.

23. Bioglass surfaces implanted in rat femur cortical bone have been studied with Auger electron spectroscopy and ion milling. The existence of the calcium phosphate layer over the silica-rich gel, similar to what was found in vitro, has been confirmed. Organic constituents, C and N, were found in the calcium phosphate layer to a depth of 180 nm, resulting in a smooth transition between an organic composition at the outer surface to a composite organic-calcium phosphate layer that overlaps the silica-rich gel on the bioglass surface.

24. In vitro solubility studies show that crystallization does not significantly affect the rate of surface ion release from the bioglass-ceramics. Implants of identical specimens in rat cortices also show interfacial bonding of bone to the implant irrespective of degree of crystallinity. This correlation shows for the first time that it is interfacial chemical variables that control ultrastructural compatibility of implants with bone rather than crystallographic or microstructural features of the implants.

25. Histological analyses of the tissue reactions at the interface of the 45S5F flame sprayed monkey hip prostheses show the absence of migration of metal particles into the tissue surrounding the implant with the bioglass coating. In contrast, the tissues around a surgical stainless steel screw of the same metal composition, without the bioglass coating, have been examined after an equivalent implantation time and show massive migration of metallic deposits into the tissues.

26. Sintered glasses and sintered composites behaved quite differently than the bulk bioglasses. Necrosis and mineralization of the surrounding tissues was seen, and by 12 months the implants had become soft and friable. This reaction probably resulted from the microporosity of the glasses with an increased surface area for reaction with the surrounding tissues and fluids.

27. Physiological dosages of parathyroid extract given to rats for 72 hours prior to sacrifice have not evoked an osteoclastic resorption at the interface of the bioglass-ceramic materials.

28. Human and chick fibroblastic tissue cultures exposed to glass-ceramic compositions (45S5F, 45B₅S5 and 45S5) were fed and maintained under physiological conditions for periods of two and three weeks on bioglass substrates. During that time the cells were observed to attach to all of these bioglass-ceramic compositions and in some instances to multiply normally. A desensitization of the bioglass surface involving equilibration to solutions of tissue culture media is required to achieve maximum tissue culture compatibility.

29. Implants of the glass-ceramics of the 45S5F composition in the vastus lateralis muscle of the right hind leg of rats showed a fibrous tissue response with the tissues firmly adhering to the implant surface. The reactions to the implants can be interpreted to show early synovial cell type formation about the implant. It can be demonstrated that this cell layer is involved in phagocytosis of the implant.

30. Comparison of other glass-ceramic compositions, 45S5 and 45B₅S5, in rat muscle showed that the more surface-reactive implant materials induced a more marked foreign body type reaction with multinucleated phagocytic cells attempting to destroy the implant. This general behavior is in marked contrast to that observed for the implant responses on bone. In bone, the more reactive glass surfaces induced osteoblastic formation and development of a chemical bone.

31. Implantation of metal and alumina canine fibular implants coated with bioglass with no internal immobilization led to non-unions of the artificial bone grafts, despite the encapsulation of the ends of the implants in generous callus. The implication is that the mechanism of bond formation depends on a sequence of events, and interruption of the sequence related to motion of the implant inhibits bond formation.

Mechanical Testing of the Bone-Bioglass Interface

32. Methods used for the mechanical testing of implants and implant-bone systems include a rapid loading torsional tester, a biaxial flexure test for disks of materials and a four-point loading bend test. A simple method for attaching strain gages to bone for the measurement of mechanical properties during mechanical loading has been accomplished.

33. A set of computer programs has been developed which allows the computation of torsional and bending stresses in arbitrary multiply-connected cross sections. The programs are user oriented, and allow a quite flexible input data structure. The program has been tested using certain configurations for which analytical stress distributions are available and has demonstrated accuracy to within five percent of the calculated value.

34. It has been shown that sufficient strength is developed at the interface of a bioglass-ceramic segmental bone replacement that a rat femur will fracture in the bone in torsion rather than at the materials-bone interface.

35. Biomechanical evaluation of femoral segmental replacements in primates has shown that the bond developed between the 45S5 bioglass-ceramic implants and bone was strong enough to cause the fracture developed in a torsional test to pass through the implant as well as the surrounding bone and the interface. This demonstrates that the bond strength is quite substantial. This type of strength has not been found in stainless steel implants flame sprayed with the 45S5F composition due to failure of the bioglass-metal interface.

36. An in vivo proof test for the ability of biomaterial to bond to bone has been developed. Small rectangular samples of the test material are implanted in rat tibiae and, after sacrifice at 10 or 30 days, subjected to a push-out force of 30 N. Implants which exhibit no gross motion due to this load are deemed bonded to bone.

37. The push-out test described above has been applied routinely to all materials undergoing implantation studies. This assures that any bonding failures are due to factors such as design of the implant or lack of fixation, rather than the chemical formulation of the material.

38. A partial hip prosthesis combining high strength mechanical behavior and controlled biocompatibility has been achieved on an exploratory scale by flame spray coating the 45S5F bioglass on 316L surgical stainless steel monkey hip prostheses. The hip prostheses have been evaluated in primate after a one-year implantation and show stable fixation in the intramedullary canal without the use of screws, cement, or any other means of mechanical fixation.

39. Fatigue studies of flame sprayed specimens show that stress and life are inversely related in a manner quite similar to that shown by

ferrous materials. Specimens tested while submerged in distilled water exhibit a lower fatigue life than specimens tested dry. The wet specimens, however, exhibited much smaller cracks once failure began than the dry specimens.

40. In studies of the torsional strength of paired bones from three groups of animals it has been shown that there is no significant left-right bias in the measured strength, and that the standard deviation of the percent difference side-to-side strength is typically about 0.10.

41. Evaluation of implants, particularly after failure of the device, requires that biomechanical factors be studied as intensively as the composition and behavior of the material.

IV. CUMULATIVE LIST OF PUBLICATIONS
RESULTING FROM THE CONTRACT

1. L. L. Hench, R. J. Splinter, W. C. Allen and T. K. Greenlee, Jr., "Bonding Mechanisms at the Interface of Ceramic Prosthetic Materials," J. Biomed. Mater. Res. Symp., No. 2, Interscience, New York, 1972, pp. 117-141.
 2. C. A. Beckham, T. K. Greenlee, Jr., and A. R. Crebo, J. Calcified Tissue Res., 8 [2] (1971).
 3. G. Piotrowski and G. A. Wilcox, "The STRESS Program: A Computer Program for the Analysis of Stresses in Long Bones," J. Biomech., 4, 497-506 (1971).
 4. T. K. Greenlee, Jr., C. A. Beckham, A. R. Crebo and J. C. Malmborg, J. Biomed. Mat. Res., 6, 244 (1972).
 5. L. L. Hench and H. A. Paschall, "Direct Chemical Bonding Between Bio-Active Glass-Ceramic Materials and Bone," J. Biomed. Mater. Res. Symp., No. 4 (1973) 25-42.
 6. B. A. Hartwig and L. L. Hench, "The Epitaxy of Poly-L-Alanine on L-Quartz and a Glass-Ceramic," J. Biomed. Mat. Res., 6 [5], 413-424 (1972).
 7. L. L. Hench, "Factors in Protein-Mineral Epitaxy," in Urolithiasis: Physical Aspects, B. Finlayson, L. L. Hench and L. H. Smith, eds., National Academy of Sciences, Washington, D. C. (1972), pp. 203-215.
 8. L. L. Hench, T. K. Greenlee, J., W. C. Allen and G. Piotrowski, "An Investigation of Bonding Mechanisms at the Interface of a Prosthetic Material," Reports #1, #2, #3, #4, #5, and #6, U. S. Army Research and Development Command, Contract No. DADA17-70-C-0001 (1970, 1971, 1972, 1973, 1974, and 1975).
 9. L. L. Hench, "Ceramics, Glass and Composites in Medicine," Medical Instrumentation, 7 [2] (March-April 1973) 136-144.
 10. L. L. Hench and H. A. Paschall, "Histo-Chemical Responses at a Biomaterials Interface," J. Biomed. Mats. Res., No. 5 (Part 1) (1974) 49-64.
 11. L. L. Hench, "Factors Affecting the Physiological Interface and Ceramics," Proceedings of Surfaces and Interfaces of Glass and Ceramics, Frechette, LaCourse, Burdick, eds., Plenum Press (1974) 265-283.
 12. A. E. Clark, L. L. Hench and H. A. Paschall, "The Influence of Surface Chemistry on Implant Interface Histology: A Theoretical Basis for Implant Materials Selection," J. Biomed. Mats. Res. Symp., "Materials for Reconstructive Surgery," Clemson Univ. (1974).

13. L. L. Hench, "Biomedical Applications and Glass Corrosion," Proceedings of Xth International Congress on Glass, Kyoto, Japan (1974).
14. C. G. Pantano, Jr., A. E. Clark, Jr. and L. L. Hench, "Multilayer Corrosion Films on Glass Surfaces," J. Amer. Ceram. Soc., 57 [9] (1974) 412-413.
15. G. Piotrowski, L. L. Hench, W. C. Allen and G. J. Miller, "Mechanical Studies of the Bone-Bioglass Interfacial Bond," J. Biomed. Mats. Res. Symp., 9 [6] (1975) 47-61.
16. L. L. Hench, "Prosthetic Implant Materials," Annual Review of Materials Science, R. A. Huggins, R. H. Rube, R. W. Roberts, eds., Annual Reviews, Inc., Palo Alto, California (1975) 279-300.
17. L. L. Hench, H. A. Paschall, W. C. Allen and G. Piotrowski, "Interfacial Behavior of Ceramic Implants," National Bureau of Standards Special Publication 415, May 1975, 19-35.
18. L. L. Hench and E. C. Ethridge, "Biomaterials--The Interfacial Problem," Advances in Biomedical Engineering, J.H.U. Brown and J. F. Dickson, eds., Academic Press, N.Y. (1975) 36-139.
19. A. E. Clark, Jr., H. A. Paschall, L. L. Hench and M. S. Harrell, "Compositional Analysis of the Formation of Bone-Implant Bond," J. Biomed. Mats. Res. Symp., "Materials for Reconstructive Surgery," Clemson Univ. (1975).
20. A. E. Clark, Jr., H. A. Paschall, L. L. Hench and M. S. Harrell, "Surface Chemical Analysis of Bioglass Orthopaedic Implants," J. Biomed. Mats. Res. Symp., "Materials for Reconstructive Surgery," Clemson Univ. (1975).
21. L. L. Hench, "Ceramic Implants," Proceedings of the 15th Annual ASME Symp. on Resources Recovery, Albuquerque, New Mexico, March 6-7, 1975, pp. 197-207.
22. A. E. Clark, Jr., C. G. Pantano, Jr. and L. L. Hench, "Auger Spectroscopic Analysis of Bioglass Corrosion Films," J. Amer. Ceram. Soc., 59, [1-2] (1976) 37-39.
23. A. E. Clark, Jr. and L. L. Hench, "The Influence of P^{+3} , B^{+3} , and F^- on the Corrosion Behavior of an Invert Soda-Lime-Silica Glass," accepted by J. Amer. Ceram. Soc. (1976).
24. L. L. Hench, "Development of a New Biomaterial-Prosthetic Device," Orthopedic Mechanics, D. Ghista, ed., Academic Press, in press.
25. G. J. Miller and G. Piotrowski, A Brief Note on the Variability of the Torsional Strength of Paired Bones, J. Biomech., 7 (1974) 247-248.

26. G. Piotrowski, Clinical Biomechanics," presented to the Symposium on Retrieval and Analysis of Orthopaedic Implants, March 5, 1976 (Proceedings to be published as N.B.S. Special Publication).
27. G. J. Miller, D. C. Greenspan, G. Piotrowski and L. L. Hench, "Mechanical Evaluation of Bone-Bioglass Bonding," 8th Annual International Biomaterials Symp., April 9-13, 1976, Philadelphia, Pa.

V. REVIEW OF PROGRESS

A detailed description of the progress made in this program during the 1975-1976 contract year is presented in the form of four papers, a standard test protocol, and two progress reports.

A. Mechanical Evaluation of Bone-Bioglass Bonding, G. J. Miller,
D. C. Greenspan, G. Piotrowski and L. L. Hench

Abstract

This study compares techniques of assessing the strength of bone-implant interfaces using several testing procedures: rapid torsion of segmental bone replacements; transcortical implant "push-out" test; and a new "mini-push-out" test. The canine "push-out" study utilized 6 mm diameter by 12 mm long cylinders of stainless steel, Cr-Co alloy, dense Al_2O_3 , bioglass, bioglass ceramic, and Al_2O_3 coated with bioglass. Specimens were implanted for 16 weeks in the cortex of dog femora. At sacrifice they were axially loaded, using a self adjusting fixture. A large difference in the "push-out" force (270 N for bioglass-ceramic vs. 14 N for inert materials) was found. Inability to determine areas precluded interfacial stress computation. Qualitative comparisons of bond strength were made and a simpler test was proposed and tested. Specimens 4 mm x 4 mm x 1 mm of bioglass, Al_2O_3 coated with bioglass, and stainless steel were implanted in the proximal tibia of the rat for 10 and 30 days. At 10 days approximately 80% of the bioglass samples were bonded and at 30 days 100% were bonded. The mini-push-out test provides an economical qualitative evaluation of interfacial bond strength while quantitative data can be achieved by the torsional testing of segmental replacements.

Introduction

The mechanical strength of the bonding between bone and new implant materials, such as bioglass, is of great importance in evaluating them as candidates for application to orthopaedic devices. Piotrowski, et al. (1971) utilized the rapid torsional test developed by Burstein and Frankel (1971) to estimate a lower limit for the torsional strength of the bond between bioglass-ceramic and the bone of the rat. Similarly, Piotrowski, et al. (1975) measured the strengths of primate femurs containing bioglass segmental replacements, and used these data and the SCADS computer program (Piotrowski & Kellman, 1973) to compute the maximum interfacial stresses developed in these systems. Initial fixation of the implant was found to be of utmost importance, and in some animals (especially the rat and the rabbit) difficult to achieve. While the primate appears to be a desirable candidate for segmental replacement studies, recent studies using modified bioglasses were plagued by non-unions which were either due to inadequate fixation or lack of bonding ability of the materials used. These two effects are difficult to separate, and thus it was impossible to decide on an appropriate course of corrective action. While a successful femoral segmental implant allows accurate quantitative evaluation of the bone-bioglass bond strength, the cost of each specimen, in terms of acquisition, surgery, and post-operative care costs, is very high. Thus it became essential that a simple, inexpensive, and rapid means of assessing the in vivo bonding ability of candidate materials be developed, in order to screen materials prior to use in the more expensive test.

Nilles, et al. (1973) and Nilles and Lapitsky (1973) reported on the use of transcortical canine "push-out" test to evaluate the biocompatibility and strength of attachment of porous implant materials.

Utilizing such a canine model results in some savings in animal costs over the primate model. However, the preparation of the specimens for subsequent testing at harvest is quite extensive. A more serious deficiency is the lack of definition of the interfacial bonding area, making an accurate computation of the shear stresses at failure impossible. Qualitative comparative data can be obtained from this method as shown in the study below, but quantitative results are extremely difficult to attain.

A modified form of the push-out test, using rats as experimental animals was evolved. Rectangular test coupons were used, and subjected to a proof load. Specimens withstanding this proof load without disruption of the bone-implant interface were judged to have the ability to bond to bone.

These techniques are compared in the following report.

Methods

Primate Model (Torsional Test) (Piotrowski, *et al.* 1975): Short segments of the right femurs of squirrel monkeys were excised and replaced by hollow cylinders made from bioglass-ceramic. Fixation during the healing process was achieved with intramedullary nails, which were removed prior to testing. The femurs were harvested after sufficient time had passed to ensure that healing had taken place, and tested to failure in torsion using the instrumentation developed by Burstein and Frankel (1971). The broken bone was reassembled and sectioned, and the stresses at each cross section computed using the SCADS computer program (Piotrowski & Kellman, 1973). Since few fractures occurred at the bone-bioglass interface, the computed stress values represent a lower limit on the strength of the interface.

Canine Model (Push-Out Test): Right circular cylindrical test coupons (6.3 mm dia. x 12.5 mm long) were fabricated from the following materials:

1. 316L stainless steel (Zimmer USA, Warsaw, Ind.)--5 samples
2. Wrought Cobalt-Chromium Surgical Alloy (Vitallium-Howmedica, Rutherford, N. J.)--4 samples
3. Al_2O_3 (99% fully dense) (Friedrichsfeld GmbH., Germany)--4 samples
4. Al_2O_3 coated with bioglass (Greenspan, *et al.* 1975)--6 samples
5. Bulk bioglass (45S5) (Hench, *et al.* 1972)--15 samples
6. Bulk bioglass ceramic (45S5C) (Hench, *et al.* 1972)--5 samples

Implantation was carried out using techniques similar to those cited by Nilles, *et al.* (1973), and the relevant portions of ASTM F361 (1975). Implants were gas sterilized, and inserted in transverse holes drilled in the lateral cortex of the femurs of mongrel dogs weighing 20-30 kg using sterile surgical procedure. At sixteen weeks the femurs were harvested (Figure 1a), sectioned (Figure 1b), and machined to form test specimens as shown in Figure 1c. The bones were kept moist throughout processing using saline solution.

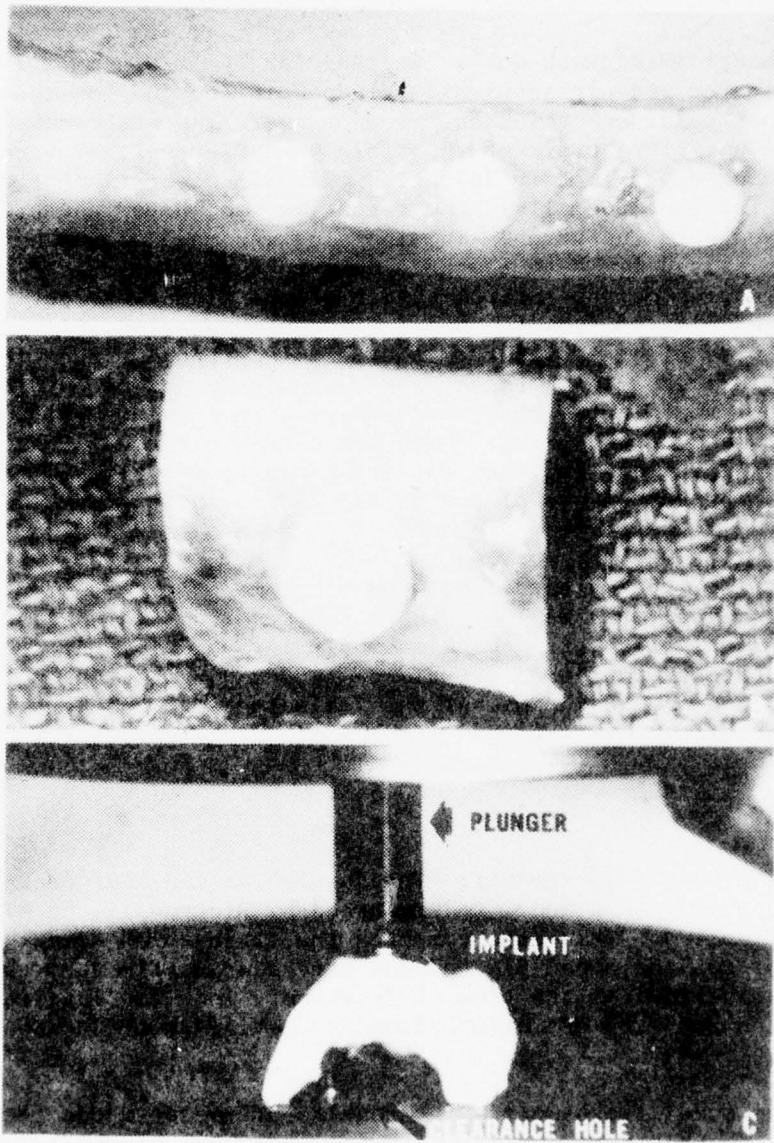


Fig. 1. Excised femur from canine push-out study with soft tissue removed (A), transversely sectioned into individual coupons (B), and machined and placed in the test fixture (C).

A self-aligning test fixture was fabricated to ensure purely axial loading of the specimens. The fixture was mounted in an Instron Universal Testing Machine and the specimens were loaded at a rate of 1.27 mm/min (0.05 in/min). The force-deflection curves were recorded and the failure loads read from those curves.

Rat Model (Mini-Push-Out): Rectangular (4 mm x 4 mm x 1 mm) implants were fabricated and ultrasonically cleaned in acetone for two minutes to remove superficial contaminants. Coupons were gas sterilized and implanted across the anterior border of the tibia (see Figure 2) of Sprague Dawley rats weighing approximately 300 gr. After administration of anesthesia (Nembutal interperitoneally), the rat's leg was shaved and prepped with alcohol and betadine scrub. The incision was made on the anterior surface of the leg from 5 mm above the knee down to the curve of the ankle. The peroneal muscles on the lateral aspect of the tibia were cut just below the knee and cleared from the bone. The anterior tibialis and common toe extensors were also removed from the medial portion of the tibia. A Hall II* drill, driven with nitrogen, was used with a 0.7 mm carbide tip burr. A slot was formed in the lateral cortex and then the medial cortex of the anterior border of the tibia. Care was taken to form a close fit without excessive clearance. The site was irrigated at all times with saline solution. The coupon was placed in the defect and the muscles and skin sutured.

A total of 80 implantations were performed; (62-45S5 Bioglass, 6-Al₂O₃, 6-Stainless Steel, and 6-Al₂O₃ double coated with Bioglass). Half of each type were implanted for 10 days and half for 30 days. At sacrifice the tibia was excised, and the soft tissue surrounding the implant site was carefully removed. Each implant was subjected to a push-out force applied with a modified sponge forceps (Figure 3a and b), designed to apply a load of approximately 30 N (see Appendix A).

Results

Primate Model (Torsional): The results of the most recent studies carried out using this model and reported by Piotrowski, et al. (1975) are shown in Figure 4. This data compares the strength of normal bone (A), strength of healing bone (B), and the stresses sustained by the bone-bio-glass interface (C) at the time of fracture. The mean interfacial stress was computed to be 83 MPa with a Standard Deviation of 23 MPa (28% of the mean).

Canine Model (Push-Out): The results of the push-out test are summarized by the histogram of the push-out forces in Figure 5. Table 1 shows the mean forces (\bar{F}), numbers of samples (n), and best estimates of the standard deviations (S.D.) for each material used. Table 2, outlines statistical comparisons between groups of specimens. Two dogs containing the bulk bio-glass specimens and several of the other materials, as noted in Figure 5, sustained femoral fractures and were sacrificed at 28 days.

*Zimmer USA, Warsaw, Ind.

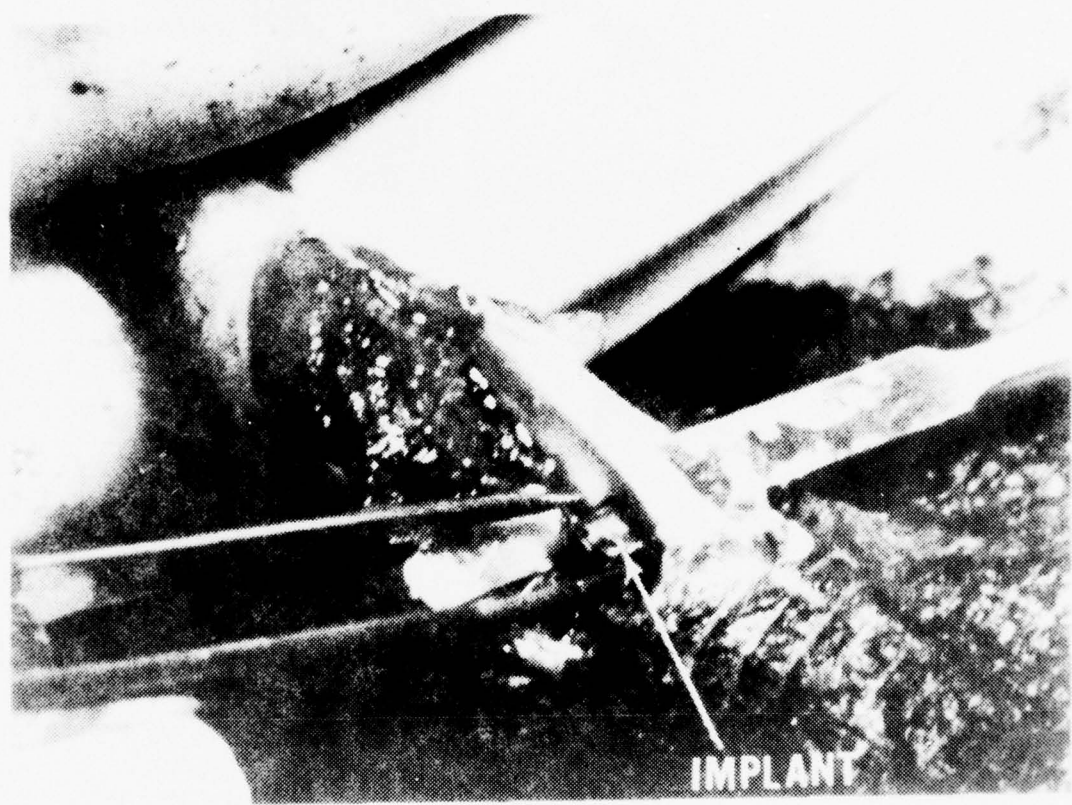


Fig. 2. Implantation of test coupon into the anterior border of the rat tibia for the mini-push-out test.



Fig. 3. Excised rat tibia, soft tissue removed, placed in the mini-push-out loading forceps.

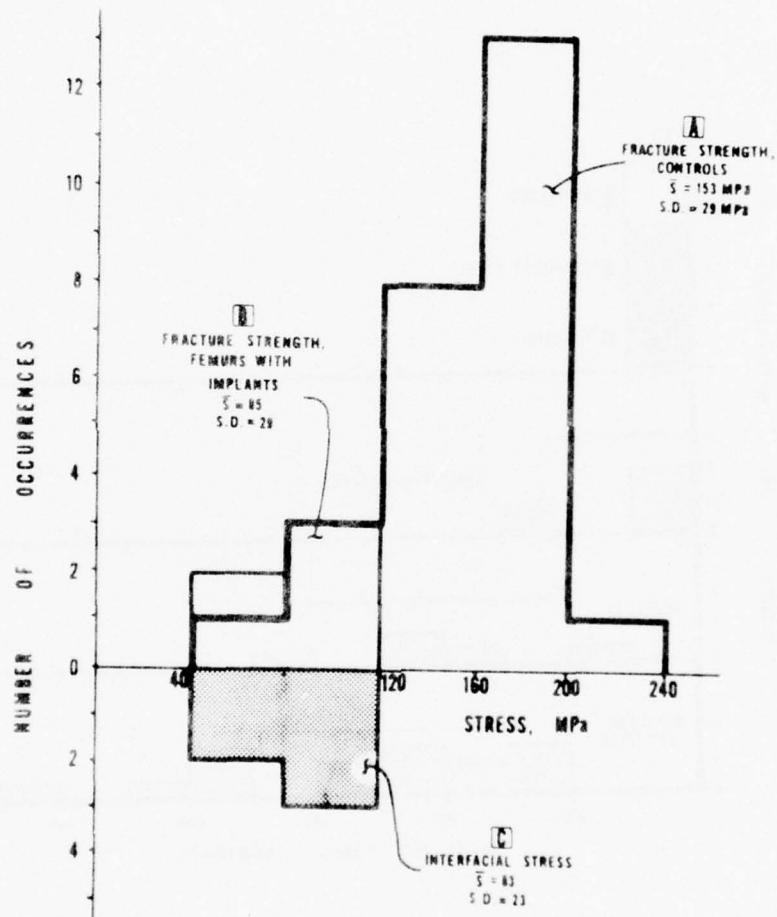


Fig. 4. Torsional strength data for primate model illustrating the fracture strength of the control groups (A), the strength of the osteosyntheses which fractured away from the implant (B) and the calculated interfacial stresses at the implant at fracture (C).

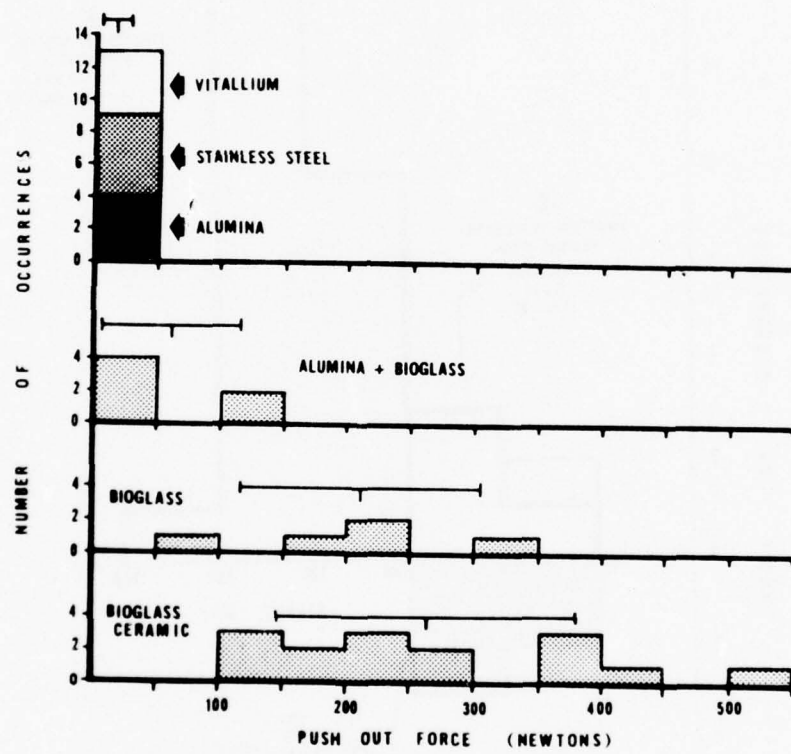


Fig. 5. Histogram summarizing the forces to push out the various compositions tested using the canine model. Except for the bioglass specimens, one specimen from each group was tested at 28 days due to fracture of one of the femurs. All of the bioglass specimens were tested at 28 days for the same reason.

TABLE 1
Canine Push-Out Data Summary

Materials	No. of Samples	Mean Force (N)	Std. Deviation* (N)
Stainless Steel - 316L**	5	12	13
Co-Cr Surgical Alloy***	4	13	11
Al_2O_3 (99% fully dense)	4	19	4
Al_2O_3 w/Single Bioglass Coating	6	61	54
Bulk Bioglass Ceramic	15	262	117
Bulk Bioglass	5	209	92

*Bessel Correction applied.
**Zimmer USA, Warsaw, Ind.
***Vitallium^R Howmedica, Rutherford, N.J.

TABLE 2
Statistical Results (Student's t Test)
Determined for the Canine Push-Out Data

Non-Bonding Materials vs. Non-Bonding Materials:

S. S. vs. Vitallium	$t = 0.1$	$P > 0.8$	$F = 1.28$
Vitallium vs. Al_2O_3	$t = 0.2$	$P > 0.8$	$F = 1.7$
Al_2O_3 vs. S.S.	$t = 0.3$	$P \approx 0.8$	$F = 1.4$

Non-Bonding Materials vs. Bonding Materials:

N.B. vs. 45S5C	$t = 8$	$P > 0.001$	$F = 90$
N.B. vs. 45S5	$t = 8$	$P < 0.001$	$F = 56$
N.B. vs. Al_2O_3 + Bioglass	$t = 3.2$	$P > 0.010$	$F = 19$

Bonding Material vs. Bonding Material:

45S5C vs. 45S5	$t = 0.9$	$P > 0.20$	$F = 1.6$
45S5 vs. Al_2O_3 + Bioglass	$t = 3.0$	$P < 0.02$	$F = 3.0$

Note: The student's t test assesses the significance of the difference of two means, while the F test compares the variances of the two groups. "P" is the probability of the two groups being represented by the same distribution.

There was no significant difference found between the mean forces required to push out inert specimens. The data from these three groups were then pooled to form a basis for comparison of non-bonding (N.B.) materials to bonding materials. The pooled data resulted in a mean force, \bar{F} , of 13.5 N (S.D. = 12 N, n = 14).

Comparison of the non-bonding and bonding materials, Table 2, showed that there was a statistically significant difference in the bond strength of the non-bonding materials and the bonding materials and that there was no significant difference between bioglass with or without crystallization (bioglass-ceramic) even though the bulk bioglass was only *in situ* for 28 days. There also was a "probably significant" difference between the bond strength of the alumina single coated with bioglass, and the bulk bioglass and bioglass-ceramic.

Rat Model (Mini-Push-Out): Of 30 specimens of 45S5 bioglass tested at 10 days, 22 specimens, representing 73% of the implants, sustained the proof load of 30 N with no visible loosening of the implant. At the 30 day time period 30 of 30, or 100%, passed the proof test. The Al_2O_3 double coated with bioglass showed 0 of 3 at 10 days and 3 of 3 at 30 days passed screening. The controls (Stainless Steel and Al_2O_3) showed no bonding and pushed out at substantially less than 30 N.

Discussion

The main detrimental feature of both types of push-out tests (dog and rat model) lies in the fact that they are subject to many interferences, especially taper, alignment and surface roughness of the specimen. Clearly, if the test coupon is tapered, close apposition of bony tissue to the implant will produce an interference fit if the implant is pushed from the larger end of the taper. This source of error can fortunately be eliminated by careful attention to implant geometry. A second factor, which is also controllable, is the orientation of the push-out force relative to the implant surfaces. The errors produced by misalignment of the force are related to the angle of that misalignment, and can be controlled by careful mounting of the test specimens in the self-aligning test fixture.

A third factor, which is more difficult to control, is the surface roughness of the implant. The surface roughness of the various specimens used in the canine studies was measured with a Brush Surface Measuring System (Model MS-5000)*, (Table 3) and the results for the inert materials are not reflected in a corresponding variation of the push-out force, indicating that the surface roughness plays a minor role in determining the push-out force.

Force intensity or interfacial shear stress could not be calculated in this investigation because an adequate measure of the true contact area could not readily be made using X-ray or microscopic observation. A nominal area could be estimated but did not appear to vary from sample to sample or material to material. The inability to calculate a force intensity or stress clearly was a major contributor to the large scatter observed in this test method.

*Clevite Corporation

TABLE 3

Arithmetic Average of Surface Roughness of Canine Implants

316L Stainless Steel	0.1 μm (4 μin)
Vitallium	1.0 μm (40 μin)
Al_2O_3	0.9 μm (35 μin)
45S5C & 45S5	0.1 μm (4 μin)
Al_2O_3 + Single Coated Bioglass	0.2 μm (8 μin)

Note: A waviness cut-off of 0.7 mm (0.3 in.) was used in determining these values.

The standard deviations, indicative of scatter in the data, ranged from a high of 90% of the mean force for the non-bonding materials to 45% for the two types of bioglass tested. The single coated alumina showed a S.D. of 88% of the mean.

The data does, however, lend itself to qualitative or comparative interpretation. As Figure 5 shows, non-bonding materials needed only small forces to push them out as compared to the bonding materials. In the canine model the dividing line seems to be at about 75 N, and thus it appears that a proof load of approximately 75 N serves to screen materials for bonding. That is, an implant of comparable size which cannot sustain 75 N push-out force can be considered to have failed the bond screening test and one which does sustain this load can be assumed to have passed and thus become a candidate material for further quantitative study.

The presence of a distinct demarcation between push-out forces for inert versus bonding materials led to the development of the rat mini-push-out test as a "go-no go" assessment of the bonding ability of a candidate material. An implant of a given material of approximately half the gross surface area was found to sustain approximately half the load to push-out in the rat model in a much shorter time period (10-30 days in rats vs. 16 weeks in dogs). Rather than utilize a large testing machine, a simply modified sponge forceps is used to provide this force, and the results correlate extremely well with the findings of the canine model. These ~~savings~~ of time and equipment resulted in comparative cost differences of twenty to thirty dollars per dog implant vs. about eight dollars per rat implant with little compromise in the usable data obtained. Quantitative data obtained using the monkey segmental model necessitates expenditures in excess of \$350.00 per implant.

Conclusion

It has been shown that the problems of estimating the area of bonding relegates the push-out method of material comparison in canines to that of a qualitative test only. The rat model provides similar data at a significant saving of time and money and appears to be easily applied and repeatable. More sophisticated models like the femoral segmental replacements in monkeys need to be carried out if quantitative data on bond strength is required. Prior screening of the materials using the mini-push-out test as an in vivo proof test, however, greatly improves the success rate of the more expensive procedures.

References

1. American Society for Testing and Materials, F361-72, "Standard Recommended Practice for Experimental Testing for Biological Compatibility of Metals for Surgical Implants," Part 46, 1975 Annual Book of ASTM Standards.
2. Burstein, A. H., V. H. Frankel, "A Standard Test for Laboratory Animal Bone," J. Biomech., 4, p. 155 (1971).
3. Greenspan, D. C., L. L. Hench, "Chemical and Mechanical Behavior of Coated Alumina," J. Biomed. Mats. Res. Symposium, "Materials for Reconstructive Surgery," Clemson University (1975).
4. Hench, L. L., Splinter, R. J., Greenlee, T. K. and Allen, W. C., J. Biomed. Mats. Res. Symposium, No. 2, Interscience, New York, pp. 117-143 (1972).
5. Nilles, J. L., J. M. Colletti, Jr., C. Wilson, "Biomechanical Evaluation of Bone-Porous Material Interfaces," J. Biomed. Mater. Res., 7, p. 231 (1973).
6. Nilles, J. L., M. Lapitsky, "Biomechanical Investigations of Bone-Porous Carbon and Porous Metal Interfaces," J. Biomed. Mater. Res. Symposium, No. 4, p. 63 (1973).
7. Piotrowski, G., R. del Valle, B. D. Miller, "The Mechanical Strength of the Bone-Ceramic Bond," in Report No. 2, "An Investigation of Bonding Mechanisms at the Interface of a Prosthetic Material," U.S. Army Medical Research and Development Command, Contract No. DADA 17-70-C-0001 (1971).
8. Piotrowski, G., L. L. Hench, W. C. Allen, G. Miller, "Mechanical Studies of the Bone-Bioglass Interfacial Bond," Sixth Annual Int. Biomaterials Symposium, J. Biomed. Mater. Res. Symp., No. 6, pp. 47-61 (1975).

9. Piotrowski, G., G. I. Kellman, "A Stress Calculator for Arbitrarily Drawn Sections--The SCADS Computer Program," in Report No. 4, "An Investigation of Bonding Mechanisms at the Interface of a Prosthetic Material," U. S. Army Medical Research and Development Command, Contract No. DADA 17-70-C-0001 (1973).
10. Piotrowski, G., G. A. Wilcox, "The STRESS Program: A Computer Program for the Analysis of Stresses in Long Bones," J. Biomechanics, 4 (6): 497 (1971).

APPENDIX A: Fabrication and Calibration of Loading Forceps

A standard sponge forceps was modified to allow for application of the rat proof load. The "sponge end" was machined to allow for clearance of the pushed out implant and a zero adjustment screw was added (Figures 3a and 3b). The forceps ratchet was placed in the first position (Figure 6). A small cylindrical block of wood was placed at the sponge end. The zero adjustment screw was brought into contact with the block. The handles were placed in a compression testing machine and load was slowly applied at points A (Figure 7). As each of the remaining ratchet positions were engaged, the load, L_H , was recorded. Using the principal of levers, the load at point B, L_I , was calculated using the equation ($L_I \times b = L_H \times a$). At the fourth ratchet position L_I was calculated to be approximately 30 N.

Acknowledgments

This study was supported through a research contract, No. DADA 17-70-C-0001, from the U.S. Army Medical Research and Development Command. The assistance of Messrs. T. C. Carr and M. Ferrari, Ms. D. Schneider, Ms. M. Harrell and Drs. H. Paschall and W. C. Allen are also acknowledged.

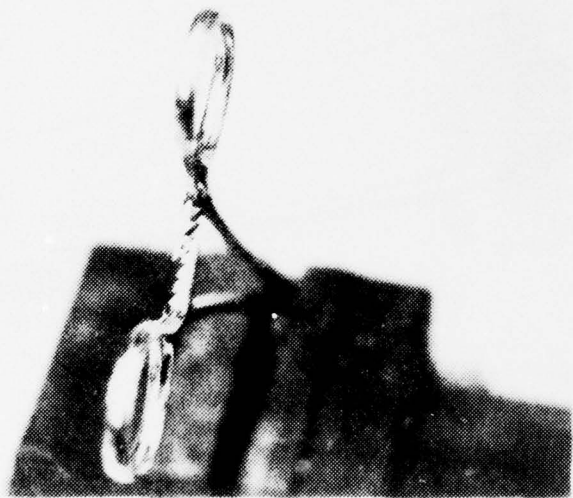


Fig. 6. Ratchet configuration of the sponge forceps in the zeroing (first) position.

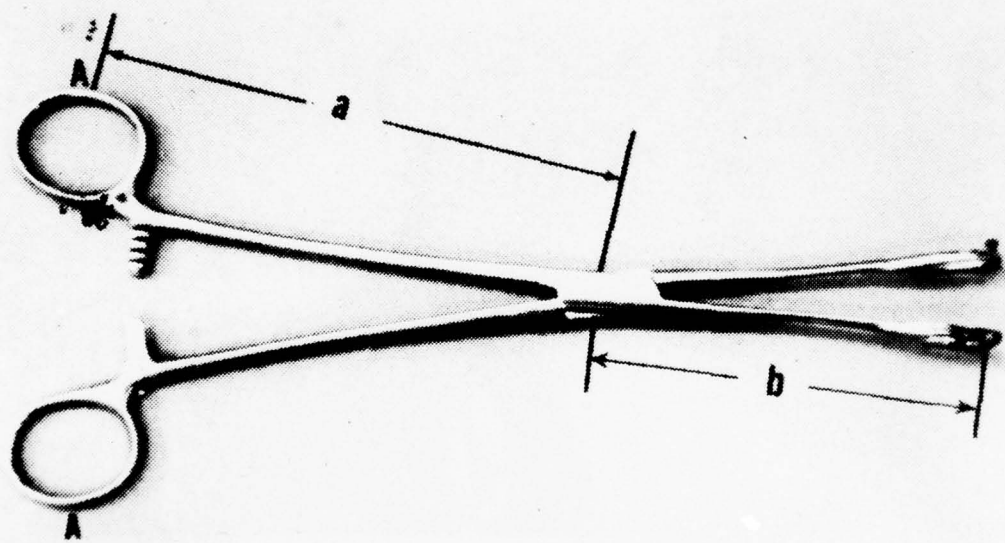


Fig. 7. Sponge forceps showing the lengths used during calibration.

B. Standard Method of Test for Ability of a Biomaterial to Bond to Bone, M. G. Ferrari, T. Carr, and G. Piotrowski

1. Scope

1.1 This procedure, developed and performed by the University of Florida Biomechanical Laboratory, is currently being used to evaluate the bonding ability of specific compositions of biomaterials. Samples of the material are surgically implanted into rat tibias and later tested for their adherence to bone.

1.2 This test is intended as an in vivo "go--no-go" test of bonding ability and cannot be used to measure or quantize different strength or rates of bonding.

2. Summary of Method

2.1 The specimen in the form of a rectangular chip is implanted in the left tibia of a rat for a period of 10 or 30 days. At sacrifice the tibia is removed, and a forceps is used to apply a force of about 30 N (6.5 lbf) on the implant. If the chip can withstand the applied force and remain fixed to the bone, the material is considered to be able to bond to bone.

3. Significance

3.1 This procedure provides a relatively rapid test of whether a given material does or does not bond to bone.

3.2 Materials that pass the test can be confidently used in other, more expensive implant studies.

3.3 Since the test employs a fixed time period and fixed push-out forces, it cannot be used to compare rates of various bone-bonding materials.

3.4 This test cannot be used to assess the bonding strength, since the load carrying area cannot be determined.

4. Apparatus

4.1 A hole is drilled in one jaw of a 9 in. sponge holding forceps in the upper-middle segment and tapped for a #2-56 screw. A 5 mm section is cut from the opposite jaw. The handle of this side is placed in a vise allowing the other handle to open and close freely. This device is used to apply the push-out force to the test specimen (see Figure 1).

4.2 Ten centimeter long burrs, 0.7 and 0.9 mm in diameter, are reduced to 4 cm and are used to machine a hole in the tibia for the implant.

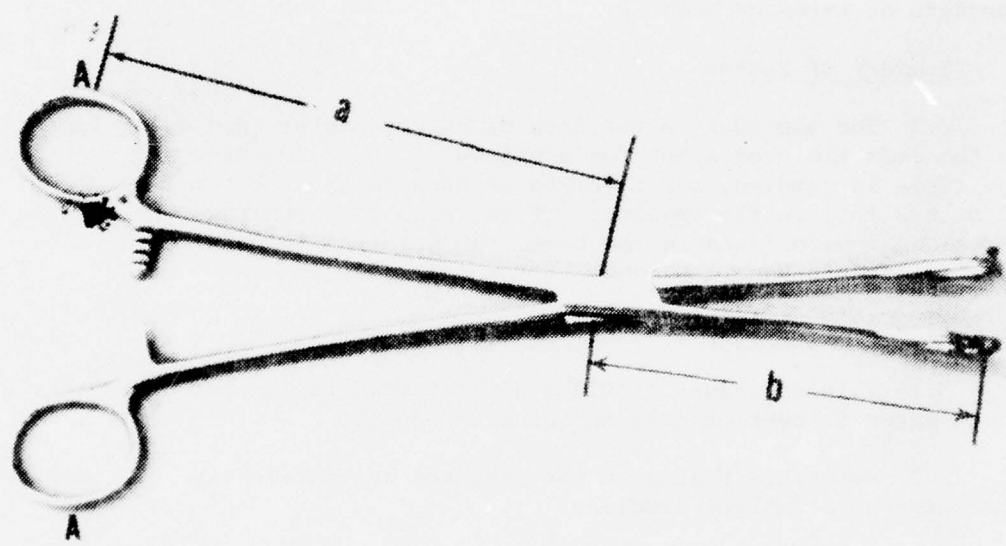


Fig. 1. The modified sponge forcep is used to apply the push-out force to the test specimen after sacrifice.

5. Reagents and Materials

5.1 The following materials are used in the preparation of the specimen for implantation.

5.1.1 Acetone

5.1.2 Vegetable parchment paper

5.1.3 Ethylene oxide indicator tape

5.1.4 Gauze pads, 4 in. x 4 in.

5.1.5 Forceps

5.2 The following materials are used in the surgical procedures involved in the implantation and sacrifice.

5.2.1 Sprague-Dawley white male rats weighing 200 to 400 g.

5.2.2 Nembutal solution -- add 3.6 cc of 50 mg/ml nemutal to 26.4 cc of sterile normal saline.

5.2.3 Atropine

5.2.4 Isopropyl alcohol

5.2.5 Betadine

5.2.6 Prep blades

5.2.7 Plywood board -- approximate size is 12 in. x 12 in. x 1/2 in.

5.2.8 Rubber bands and tacks

5.2.9 Sterile surgical kit -- contains sterile drapes, applicators, gauze pads, gloves, saline solution, syringes, towel clamps, forceps, scalpels, sutures (4-0 silk and 4-0 sutures), needleholder and scissors.

5.2.10 1/4 in. periosteal elevator

5.2.11 Drill -- a nitrogen driven drill, with 0.7 and 0.9 mm carbide tipped burrs, operated at 50 psi.

6. Sampling

6.1 Three rats for each time period (10 days and 30 days) have been used in the initial studies, and this number appears to be sufficient.

6.2 If an animal sustains a broken leg or dies prior to harvest it should be replaced.

7. Test Specimens

7.1 Fabricate the biomaterials implants as rectangular parallelopipeds measuring 4 mm x 4 mm x 1 mm. All surfaces and edges shall be free of burrs and other surface irregularities which may cause a mechanical interlock with the healing bone. The surface shall be no rougher than that produced by grinding with 600 grit paper.

7.2 Clean the specimens ultrasonically in acetone for one to two minutes to remove all surface contaminants. To prevent further contamination, further handling of implants is to be done only with forceps. Wrap the implants individually in a gauze pad and vegetable parchment paper using the customary double wrapping technique, and close the package with ethylene oxide indicator tape. Mark the implant type (material) in the tape.

7.3 Sterilize the implants with ethylene oxide and aerate them for 24 hours.

8. Procedure

8.1 Preparation of animal

8.1.1 Anesthetize the rat with nembutal solution, using the dose given by Table 1, injected interperitonially. Once the anesthetic takes effect, inject 0.2 cc of atropine subcutaneously.

8.1.2 Alcohol and prep blades are used to ensure sterility when shaving the leg. Shave the leg from about an inch above the knee to the ankle and about 60 degrees to each side of the leg. Scrub the shaved region with betadine using sterile applicators. Place the rat with his back on a plywood board. The right rear leg and the two front legs are held down by rubber bands tacked into the wood. Enough tension is applied to hold the rat in place.

8.2 Surgical Procedure

8.2.1 Place a sterile paper absorbent towel over the animal and cut a diamond-shaped hole in the center. Pull the leg through the hole and again swab with betadine for precautionary measures. Use a sterile gauze pad to remove excess betadine.

8.2.2 With a #15 scalpel blade, make an anterior incision through the skin 5 mm proximal to the knee, along the length of the bone, to the curve of the ankle. Cut the two peroneal muscles on the lateral side of the tibia just below the knee, and clean them from the bone. Remove the anterior tibialis and common toe extensors from the bone on the medial side, and cut the semitendinosis. This procedure allows access to the periosteum which is removed from the medial and lateral side and the anterior ridge of the tibia. The muscles are then cleaned from the medial and lateral aspects of the bone in preparation for drilling. Insert the periosteal elevator posterior to the tibia to evaluate the tibia from the muscle. Now the bone is clear of surrounding muscles and tissue and can be drilled to receive the implant as shown in Figures 2 and 3.

TABLE 1

NEMBUTAL DOSAGE CHART

<u>Weight of rat (g)</u>	<u>Volume of nembutal solution (ml)</u>
110	0.72
120	0.78
130	0.85
140	0.91
150	0.97
160	1.04
170	1.11
180	1.17
190	1.24
200	1.30
210	1.37
220	1.43
230	1.50
240	1.56
250	1.63
260	1.69
270	1.76
280	1.82
290	1.89
300	1.95

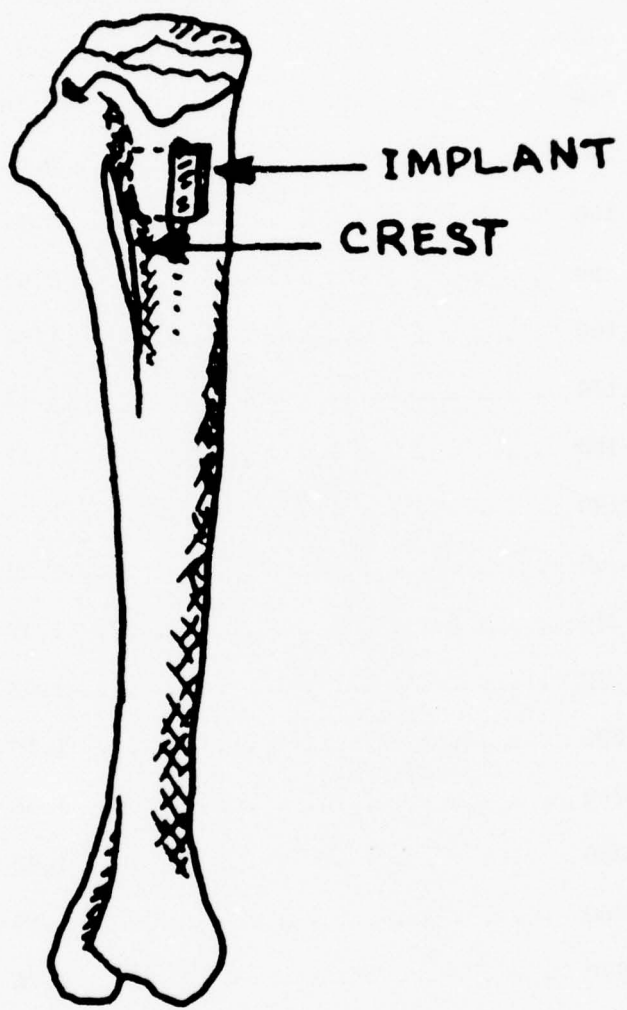


Fig. 2. The location of the implant immediately post-operatively should be immediately posterior to the tibial crest, as shown.



Fig. 3. The implant is being inserted in the defect machined into the proximal tibia. The periosteal elevator shown in the background is used to maintain the musculature around the tibia away from the implantation site.

8.2.3 Drill the tibia from the lateral to medial side. Check the width of the slot intermittently with the implant to ensure a proper fit. The implant is to fit securely into the slot in the bone so that the implant is not free to move but can be readily pushed with the fingers. Use saline solution repeatedly to irrigate the area and wash away fragments of bone.

8.2.4 Place the bioglass chip in the tibia, while checking that the implant can be removed either laterally or medially by applying a slight pressure. Rinse the implantation area one final time with a saline solution.

8.2.5 Stitch the muscle on the lateral side of the incision to the fascia of the medial side with a discontinuous stitch by understitching with chromic 4-0 suture and a tapered needle. Close the skin of the rat with a continuous stitch using silk 4-0 suture and a cutting needle and secure the final stitch with a knot.

8.3 Testing Procedure

8.3.1 At the time of testing, sacrifice the rat by intravenously injecting it with an overdose (about 5 cc) of nembutal, or some other standard procedure.

8.3.2 Remove the tibia from the rat and clean it of surrounding muscle and tissue. Any material covering the periphery of the bioglass implant is carefully removed so that only the interfacial bond strength is involved in holding the implant in place.

8.3.3 Place the tibia between the jaws of the forcep, making sure to align the adjusting screw on the forcep with the implant as in Figure 4. Some portion of the proximal end of the tibia may be removed in order to properly position the bone in the testing apparatus. Adjust and align the screw to provide essentially no clearance and no load on the implant when the forcep is closed to the first position.

8.3.4 When the forcep is closed past the first position, a force is applied to the implant. At the fourth position, a force equivalent to 30 N is applied on the implant. Close the forcep to the fourth position, taking about 5 seconds.

9. Interpretation of Results

9.1 The specimen is deemed to have passed the test, and is therefore bonded to the bone, if it survives the application of the 30 N load without visually perceptible motion taking place between bone and implant.

9.2 A biomaterial is deemed to be a bone-bonding material if all of the 30 day specimens pass the test.

9.3 A biomaterial can be assumed to be a low-bonding material if all of the 10 day specimens pass the test. The 30 day implants should still be harvested, and the bone-bonding ability confirmed according to 9.2.



Fig. 4. The adjusting screw of the modified forcep is adjusted to contact one end of the implant, while the bone is supported by the other jaw of the forcep.

10. Report

10.1 Records of the following information for all animals implanted shall be kept for future reference, if needed.

10.1.1 Material implanted.

10.1.2 Names of individuals involved in the implantation, sacrifice, and testing.

10.1.3 Amount of anesthesia administered.

10.1.4 Weights of the animal at implantation and sacrifice.

10.1.5 Dates of implantation and sacrifice.

10.1.6 Results of push-out test (passed or failed).

10.1.7 For those animals which did not result in a push out test, a reason for the lack of test data must be given.

10.2 The report shall include the following imformation.

10.2.1 Type of material.

10.2.2 Number of animals implanted for each time period.

10.2.3 Number of implants at each time period that passed the push-out test.

10.2.4 Number of implants not tested, and reasons for lack of test.

C. Material Screening for Bonding Ability, M. Walker, T. Carr,
S. Gould, and G. Piotrowski.

Introduction

The ability of bioglass to promote secure bony attachment has been well established [1, 2]. The most successful glass tested so far has been that of the 45S5 composition. The bonding ability of 45S5 bioglass has been compared over the years to controls of dense alumina, stainless steel and fused silica. All three of these inert materials have been shown to produce no significant bonding. The difference in behavior shown by fused silica (pure glassy SiO₂) vs bioglass, which is also a silicate based glass, is quite significant. It shows that bonding of a material such as bioglass to bone is determined by compositional factors. It is this dependence of bonding on composition that will be studied in this project.

Through systematic and progressive compositional variation of our standard 45S5 bioglass, limits will be determined beyond which bonding no longer occurs. This process should define a compositional range of SiO₂, P₂O₅, CaO and Na₂O in which bonding will occur. It will also establish whether all four of these components are necessary for bonding and if not, which are superfluous. The shape and limits of the composition region of bonding when plotted on a triaxial chart should provide valuable insight into the compositional factors involved in the basic mechanisms of bonding. It is possible that the determination of this acceptable compositional range will provide glasses of more suitable mechanical or fabricative properties to be employed in clinical prostheses. Glasses of greater soft tissue stability that will also bond to bone may be an added benefit from the study. Of special importance is our plan to use this study as a basis for selecting samples for the further in vivo investigations.

Initial Evaluation of the Mini-push Out Test.

Bioglass implants of varying compositions have been mechanically tested using the rat tibial mini-push out technique developed by Miller, Greenspan, Piotrowski and Hench [3]. In brief, the mechanical integrity of the bioglass-bone bond is tested in the following manner: 4 x 4 x 1 mm bioglass chips are implanted into a surgical defect wholly through the anterior border of the tibia in a sagittal plane. After a given healing period the animal is sacrificed and the tibia excised. The exposed ends of the implant on either side of the tibia are cleaned of overlying bony tissues. Modified sponge forceps are used to apply a push out load of 30 newtons to the implant. Those implants that resist being forced out under the 30 N proof load have passed this test for bonding. Those that move perceptively at 30 N or less have failed.

The first application of this in vivo proof test of bonding ability was to establish the reliability of the bond formation. Ten separate lots of 45S5 bioglass were formulated, and six rat tibia implants fabricated from each lot. Three chips of each lot were implanted for ten days, and three for thirty days, as described in the test protocol [4]. (In two cases, four implants were tested at thirty days.) The results of the proof test on a lot-by-lot basis are shown in Table I. 73% of the ten day implants were

already bonded, and the eight failures were quite randomly distributed over all ten lots. All of the thirty day implants were found to be bonded. Clearly, 45S5 bioglass consistently bonds to bone in rat tibiae in less than 30 days.

Table I
Results of Mini-push Out Test for
10 Lots of 45S5 Bioglass

Lot No.	10 Days				30 Days			
	No. of Implants	Passed	Failed	No. of Implants	Passed	Failed		
1	3	2	1	3	3	0		
2	3	3	0	4	4	0		
3	3	2	1	3	3	0		
4	3	2	1	3	3	0		
5	3	2	1	3	3	0		
6	3	3	0	3	3	0		
7	3	2	1	4	4	0		
8	3	2	1	3	3	0		
9	3	3	0	3	3	0		
10	3	1	2	3	3	0		

Material Screening Studies.

Further tests with the mini-push out test were performed to evaluate the bonding ability of other material systems and are summarized in Table 2. Inert materials, like 316L stainless steel and fully dense alumina showed no bonding ability at either time period.

Alumina coated with a single layer of bioglass showed very questionable results, and was deemed to have failed the test. Double coated alumina, as described by Greenspan and Hench [5], fared somewhat better, but the results are still not very conclusive, and the test will be repeated.

Stainless steel specimens coated with bioglass using the immersion technique described by Buscemi and Hench [6] showed good response at thirty days. The small size of the implant made it impossible to completely encapsulate the metal in glass. Instead, the implants were fabricated in the form of a sandwich, with a layer of bioglass on either side of the steel piece. The edges of the steel-glass interface were exposed to body fluids, and showed no attack or degradation at either ten or thirty days.

A series of monkey segmental replacements were tested about a year ago in an attempt to improve our knowledge of the bond strength between bioglass and bone. A minor change in the composition of the bioglass was made, however, by substituting calcium phosphate for some of the CaO, thereby obviating the need for the addition of P₂O₅ to the glass mixture. None of the monkey

implants bonded, and it was not clear whether the change in formulation, which should have no effect on the chemical composition and the behavior of the bioglass, rendered the glass incapable of bond formation, or whether there was insufficient fixation to allow the bond to form. One of the failed (i.e. unbonded) monkey segmental implants was retrieved, and two rat tibia implants were sawn from it. Both of these implants bonded at ten days, indicating that the material was capable of forming a bond to bone (at least in rat tibiae), and suggesting very strongly that lack of fixation caused failure of this series of implants. This last case illustrates very well the value of the mini-push out test, since it assesses the bonding ability of the material with very little interference from other variables, such as stresses at the interface or motion of the implant.

Table 2
Summary of Material Screening Studies

Material	10 Days			30 Days		
	No. of Implants	Passed	Failed	No. of Implants	Passed	Failed
45S5 bio-glass (see Table I)	30	22	8	32	32	0
316L Stainless Steel	3	0	3	3	0	3
Alumina, fully dense	3	0	3	3	0	3
Alumina with simple fusion coat of 45S5	14*	0	7	3**	1	1
Alumina with two fusion coatings of 45S5	3	0	3	3	2	1
316L Stainless Steel coated with 45S5	5***	2	2	2	2	0
Calcium phosphate type 45S5	2	2	0	---	---	---

*Two animals died of causes not related to implants, 5 suffered fractured tibae.

**One rat sustained a broken tibia.

***One rat died of causes not related to the implant.

Compositional Studies: Substitution of Potassium for Sodium

The bonding ability of bioglasses in which varying portions of Na₂O were replaced with K₂O was investigated. One reason for our concern for understanding the importance of the substitution of K₂O for Na₂O is the extensive tissue culture investigation of Rappaport [7] where she showed that various cultures were very compatible with glass discs containing K₂O. Her theory that this positive response was due to K⁺ ions interacting beneficially with cell membranes suggests that a similar increase in tissue compatibility should arise with bioglasses containing K₂O. The code names used for the various compositions studied with our test method are explained in Table 3. Each composition was tested in triplicate for both 10 and 30 days, and the results are summarized in Table 4.

Table 3
Compositions Used to Study Effect of Na-K Substitution

		<u>mole %</u> <u>wt. %</u>				
	<u>Code Name</u>	<u>SiO₂</u>	<u>P₂O₅</u>	<u>CaO</u>	<u>Na₂O</u>	<u>K₂O</u>
1	45S5 N	<u>46.1</u> 45.0	<u>2.6</u> 6.0	<u>26.9</u> 24.5	<u>24.4</u> 24.5	<u>0</u> 0
2	45S5 N ₃ K	<u>46.1</u> 43.6	<u>2.6</u> 5.8	<u>26.9</u> 23.8	<u>18.3</u> 17.8	<u>6.1</u> 9.0
3	45S5 NK	<u>46.1</u> 42.3	<u>2.6</u> 5.6	<u>26.9</u> 23.1	<u>12.2</u> 11.5	<u>12.2</u> 17.5
4	45S5 NK ₃	<u>46.1</u> 41.1	<u>2.6</u> 5.5	<u>26.9</u> 22.3	<u>6.1</u> 5.6	<u>18.3</u> 25.5
5	45S5 K	<u>46.1</u> 39.9	<u>2.6</u> 5.3	<u>26.9</u> 21.8	<u>0</u> 0	<u>24.4</u> 33.0

There is not major difference in the bonding ability of glasses containing various ratios of Na to K, since all of the implants unequivocably bonded at thirty days. This suggests that the role played by Na₂O is the same as that played by K₂O. The variation in results at the ten day period indicates that there may be a rate effect due to relative Na and K concentrations, but the data is too sketchy for any firm conclusions to be drawn.

Table 4
Effect on Bonding Ability of Substitution of K₂O for Na₂O

Material	No. of Implants	10 Days		30 Days	
		Passed	Failed	Passed	Failed
45S5 N	3*	1	1	3	3
45S5 N ₃ K	3	1	2	3*	2
45S5 NK	3*	0	2	3*	2
45S5 NK ₃	3*	2	0	3	3
45S5 K	3	0	3	3	0

*One animal in this group sustained a fracture of the tibia.

References

1. L.L. Hench, R.J. Splinter, W.C. Allen, and T.K. Greenlee, Jr., "Bonding Mechanisms at the Interface of Ceramic Prosthetic Materials", *J. Biomed. Mater. Res. Symp.*, No. 2, Interscience, New York, pp. 117-141 (1972).
2. G. Piotrowski, L.L. Hench, W.C. Allen, and G.J. Miller, "Mechanical Studies of the Bone-Bioglass Interfacial Bond", *J. Biomed. Mater. Res. Symp.*, No. 6, Interscience, New York, pp. 47-61 (1975).
3. G.J. Miller, D.C. Greenspan, G. Piotrowski, and L.L. Hench, "Mechanical Evaluation of Bone-Bioglass Bonding", *8th Annual Int. Biomater. Symp.*, April 9-13, Philadelphia, Pa. (1976).
4. M.G. Ferrari, T. Carr, and G. Piotrowski, "Standard Method of Test for Ability of a Biomaterial to Bond to Bone", this report, pp
5. D.C. Greenspan, and L.L. Hench, "Chemical and Mechanical Behavior of Coated Alumina", *J. Biomed. Mater. Res. Symp.*, No. 7, Interscience, New York, pp (1976).
6. P. Buscemi and L.L. Hench, "An Immersion Process for Coating Metal Implants with Bioglass:", this report, pp.
7. C. Rappaport, "Some Aspects of Growth of Mammalian Cells on Glass Surfaces", in The Chemistry of Biosurfaces, vol. 2, ch. 9, Hair, M.L., ed., Marcel Dekker, Inc., New York, 1972.

D. An Immersion Process for Coating Metal Implants With Bioglass,
by P. Buscemi and L. L. Hench

Introduction

A technique for producing bioglass-coated metal devices has been developed in the laboratory after two conventional methods for coating other glasses onto metals were shown to be unsuccessful. One method was conventional enameling with glass frits and the other was flame spraying.

The enameling method failed in this case because the high melting temperature of the glass and the time required caused an unacceptable amount of diffusion of iron into the bulk of the glass. The flame spraying method failed because the high temperatures necessary to keep the small glass particles molten vaporized sodium from the glass, causing a reaction at the metal-glass interface which produced a porosity fatal to a glass-metal seal.

To overcome these deficiencies, a promising new method has been developed. It involves the immersion of the piece to be coated into the molten bioglass for three (3) to five (5) seconds, followed by rapid cooling. The process allows the precise control of the composition of the glass on the external surface, and diffusion of metal into the glass coat is minimal.

Critical Parameters

The parameters which determine the nature of the glass-metal interface are (1) the viscosity and temperature of the glass, (2) the thermal expansion of the system, (3) the oxidation of the metal substrate and (4) the time of the process. These are more fully explained as follows.

1. Viscosity

Bioactive glasses of different compositions are melted in platinum crucibles for 3 to 12 hours to ensure homogeneity. The melting temperatures of the glasses range from 1300°C to 1550°C. Elevated alkali content decreases viscosity and promotes the diffusional properties of the glass which permits chemical bonding. By varying the temperature of the molten glass by increments of 10°C to 25°C the viscosity of the glass can be controlled. This parameter, although not affecting the chemical properties of the glass, allows coatings of various thicknesses to be applied to the metal substrate depending on how fast it is withdrawn from the melt.

2. Thermal Expansion

Instead of using multiple coatings of glass or ceramics to relieve stresses, the concept used here takes advantage of two physical properties

of metals: (1) at relatively low temperatures (below 700°C) the thermal expansion of most metals (materials) is almost linear, and (2) the time required to heat up, and thereby expand, a metal specimen is long (15-30 min.) compared to the time required for a surface layer of glass to cool from 1400°C to 700°C (less than 60 sec). Prior to immersion, the metal is heated to a temperature which causes the same expansion as that in the molten glass, relative to room temperature. Thus during the cooling process both metal and glass contract the same amount, thereby eliminating the stresses which would otherwise develop at the interface between materials of different thermal expansion coefficients. The relative temperatures and expansion are illustrated Figure 1. The rapid cooling of the glass between high (1300°C) and low (700°C) temperatures is allowed because glass flow in this region relieves local thermal strain quickly. The process itself involves a total immersion time of three (3) to five (5) seconds depending on the size of the metal substrate.

3. Oxidation of Metal Substrate

In the immersion process a relatively thick oxidation surface is created on a rough (sand blasted) metal surface. The term oxidation layer is used in the chemical sense to mean that a chemical reaction between the metal substrate and a gaseous element (which need not necessarily be oxygne) undergoes an electron transfer process to form a surface of specific characteristics. The process involves the control of temperature, time and vapor pressure of the gaseous oxidizing element to form an oxidation layer which permits chemical bonding to the bioglass through high temperature diffusion. In this manner it is the metal substrate itself which provides the transition layer to the glass. No further modification of the glass and substrate need be made.

The surface roughness of the metal substrate also controls the degree of interpenetration of the oxidation layer between the metal substrate and the glass. The roughness is not meant to provide "mechanical interlocking." Indeed, excessively rough surfaces cause residual stresses upon cooling. The control of the roughness is a means of further controlling the oxidation process. The oxidation process varies for different metals of different shapes, but as an example 20 min. at 800°C in air is required for a 316L stainless steel implant as shown in Figure 2.

4. Time

The factor of time has been mentioned in the above three sections. The time of immersion is a critical variable dependent upon type of metal substrate and glass coating.

Results

An example of a device coated with this method is shown in Figure 2. The substrate is made of 316L stainless steel and is coated with

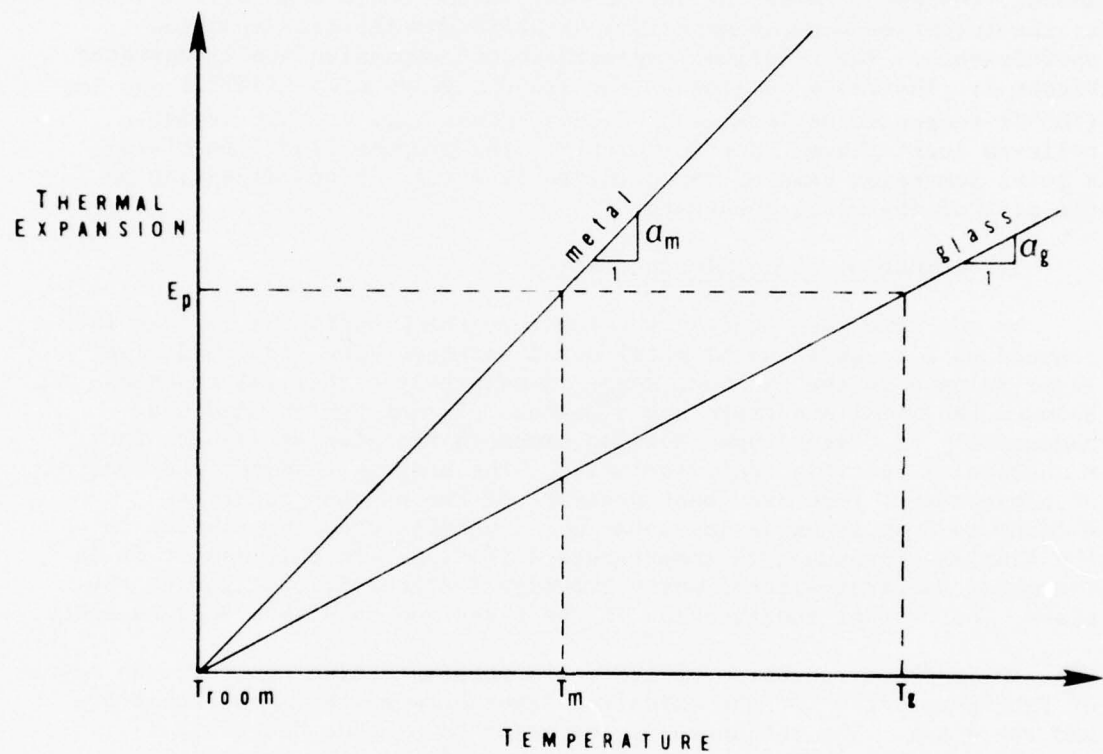


Fig. 1. The coefficient of thermal expansion of the metal, α_m , is larger than that of glass, α_g , but just prior to immersion the metal is heated to a temperature T_m such that the actual expansions of the metal and the glass are equal at E_p . The immersion time is short enough that the metal doesn't have time to heat up and expand. After immersion, both materials cool down to room temperature and contract equally.



Fig. 2. This femoral head prosthesis for a monkey was fabricated by the College of Engineering Shop and coated with the immersion process. Total length of the device is approximately 65 mm. The coating on the stem was machined by grinding to produce a uniform cross section, while the glass coating of the head was left in its natural form.

45S5 bioglass. Test pieces made by this method have been successfully tested in rats and shown to bond to bone within 30 days (3). Other test devices have withstood autoclaving (heating to about 150°C).

Figure 3A shows the interface between the glass and metal when polished to a fineness of 600 grit. The porosity, which is clearly visible, is due to the formation of the metal oxide in air rather than in a controlled atmosphere. A controlled atmosphere would produce a dense rather than porous oxide film. However, the unoptimized system of Figure 3A survives immersion in buffered solution much better than the previously tested flame sprayed devices. Figure 3B shows the bioglass-metal interface of a flame sprayed device for comparison. Large voids, frequently extending down to the metal surface, are clearly evident, and are responsible for the low strength of the glass-metal bond.

Energy dispersive X-ray analysis (see Figure 4) across 8 μm of the interface of the section shown in Figure 3A shows a transition region of approximately two (2) microns in breadth. A definite inter-diffusion of iron, chromium, calcium and silicon exists in this area, thus confirming the existence of chemical bonding. The primary method of testing the strength of this bond will involve ASTM C633, Standard Method of Test for Adhesion or Cohesive Strength of Flame-sprayed Coatings, and is currently in progress.

Other metal substrates have been coated by this method including titanium and chrome cobalt alloys. In cases where the thermal expansion of the substrate is less than the 45S5 bioglass, a modification to the composition of the glass must be made. An enclosed system for coating substrate metals in a completely controlled atmosphere does not yet exist. The capability to perform the oxidation and coating phases separately under positive pressure of argon is under development.

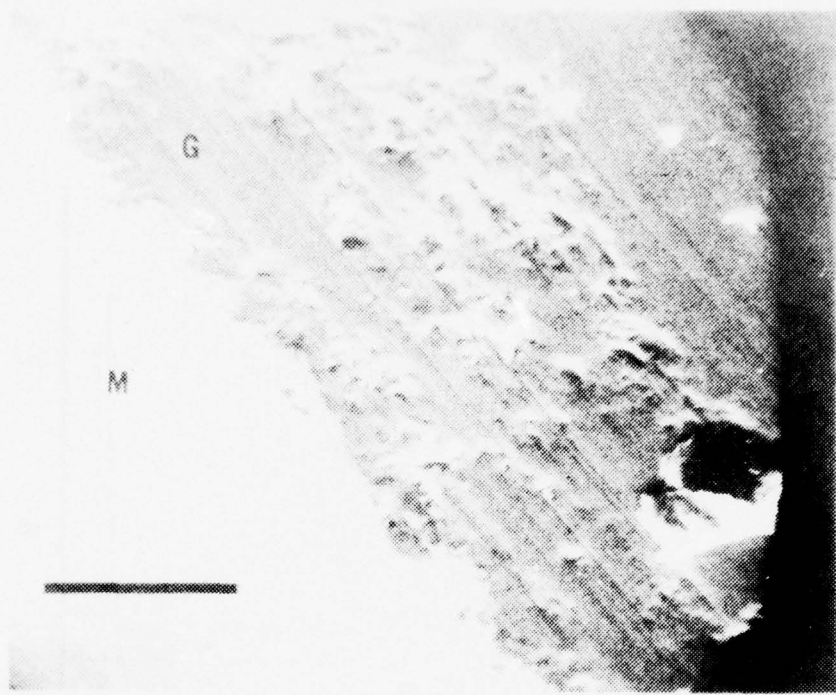


Fig. 3a. This SEM micrograph illustrates the cross section of the interface produced by immersing a 316L stainless steel piece (M) into 45S5 bioglass (G). The white bar is 50 μm long.

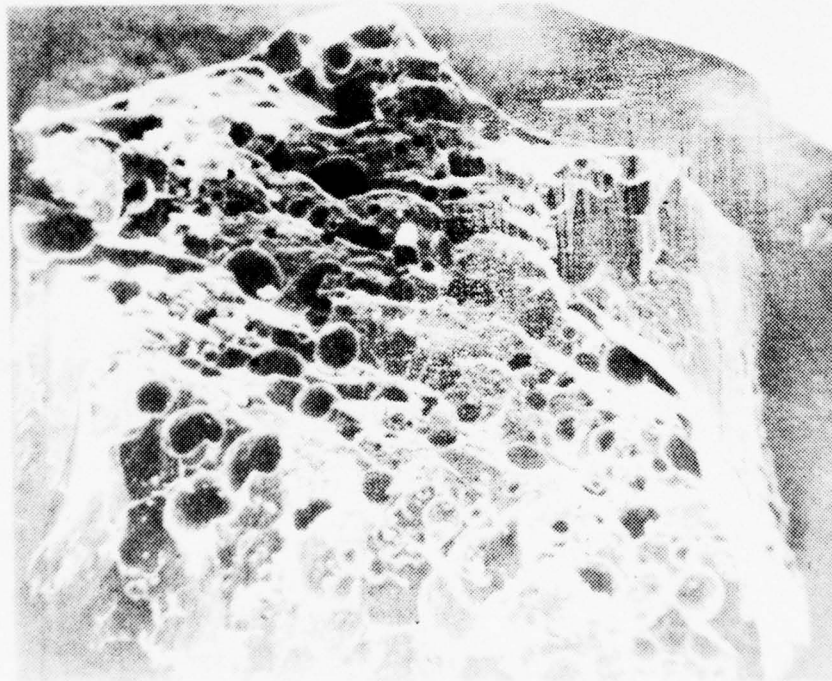


Fig. 3b. The fracture surface of 45S5 bioglass flame-sprayed onto stainless steel shows many voids, some of which penetrate to the metal. The white bar is 50 μm long.

45S5 BICGLASS

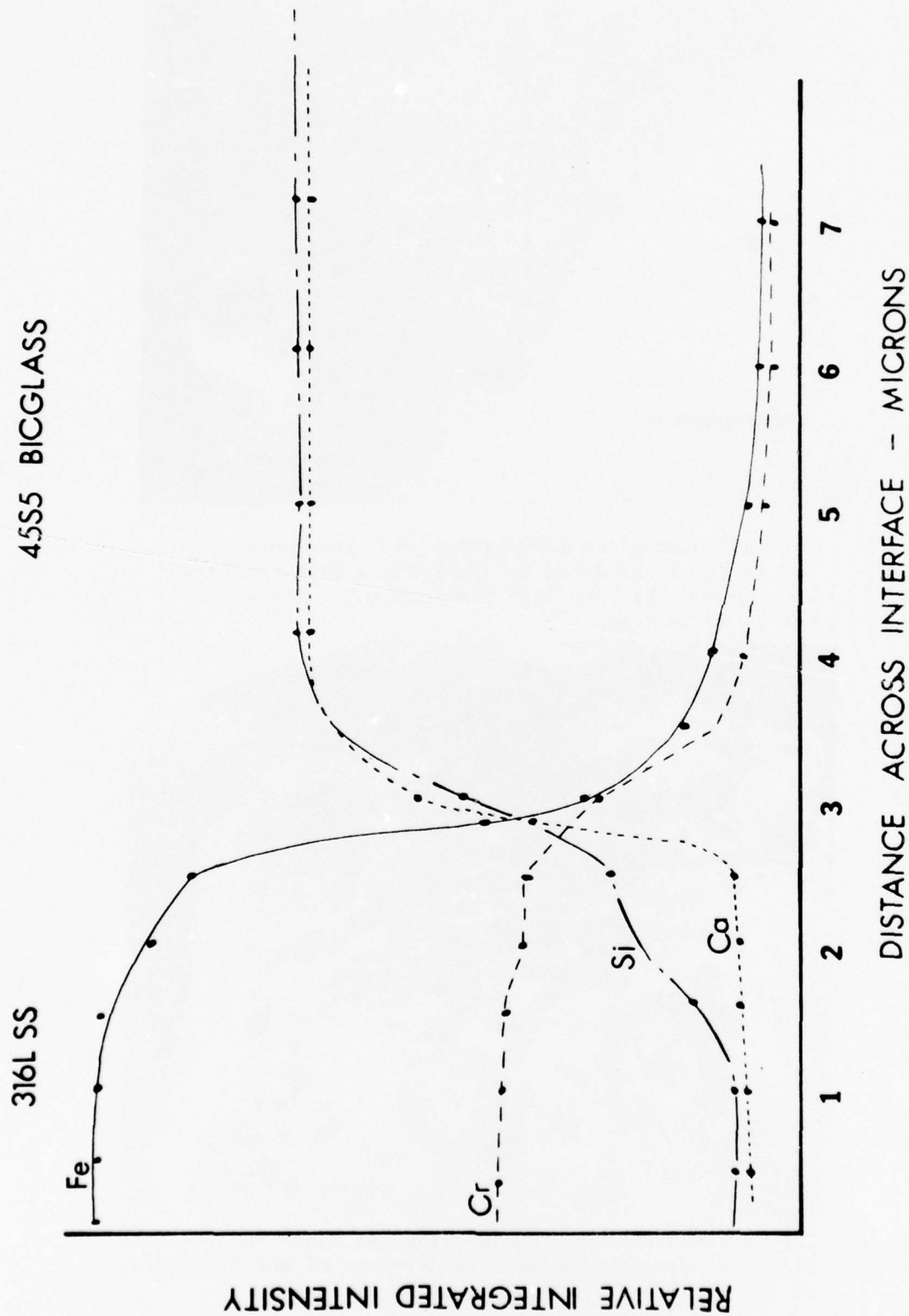


Fig. 4. Compositional analysis across the interface shown in Figure 3a shows a 2 μm wide transition region between the stainless steel and the bioglass.

E. Studies in Artificial Bone Graft Materials--A Progress Report,
G. Piotrowski, H. Burchardt, T. Carr, D. Greenspan and P. Buscemi

Introduction

The study reported herein focusses on the mechanical and macroscopic structural details of the bone-bioglass bond. Artificial replacements for segments of canine fibula were implanted and harvested at 12 and 24 weeks. The major purpose of this study is to ascertain the spatial pattern of repair in the vicinity of the implant-bone junction, the strength of the junction, and the activity level in the bone. Data obtained in this study will be compared to previous and current work at this institution with autogenous bone grafts [1] and Navy bank bone.

Methods and Materials

Six dogs were implanted for each of two time periods, 12 and 24 weeks, for each of two types of implants. One type of implant was fabricated from fully dense alumina coated with bioglass [2], and the other from 316 stainless steel coated with bioglass [3]. Each dog underwent two simultaneous graft operations. On the right hand side a 40 mm long piece of fibula was excised, frozen, and stored for subsequent testing. The defect in the bone was filled with an equally long artificial replacement. On the left side a 40 mm long segment of fibula was excised, inverted proximal to distal, and replaced. The advantage of this particular model was that no internal or external fixation devices were required to secure the implant or transplant in place, and therefore material reactions could be studied without the necessity of introducing foreign materials, such as metal fasteners. At the time of sacrifice the strength of each of the four graft-host junctions was to be tested in torsion by cutting the graft or implant in half and removing 40 mm long test specimens from each side. All five specimens (normal fibula removed at operation, two autogenous graft-host junctions, and two bioglass-bone junctions) were to be tested for each animal. Mechanically, the strength, deflection to failure, and energy absorption was to be studied. This data was to be correlated to the porosity and cumulative formation in the bone.

Post-operatively each of the dogs was fed tetracycline, an antibiotic which is deposited in newly formed bone and fluoresces under ultraviolet lighting. This allows for quantitative determining of bone formed during the post-operative period. X-rays were routinely taken at two week intervals, so that progress of healing could be followed.

Current Status of the Project

Seven implants have been harvested: 4 of 6 bioglass-alumina implants at 24 weeks, 2 of 6 bioglass-alumina implants at 12 weeks, 0 of 6 bioglass-steel implants at 24 weeks, and 1 of 6 bioglass-steel implants at 12 weeks. None of the harvested implants was bonded to the host bone. In contrast, all of the autogenous graft host junctions were healed. These graft-host junctions have been frozen and stored and will be tested mechanically when harvesting of all implants has been completed in mid-December.

The following is a typical clinical and roentgenographic history of the implant in contrast to the autograft. Within the first four weeks, a substantial amount of callus appears around the ends of both autografts and implants. The callus formation on the autograft side seems to be more extensive and is gradually incorporated to the bone on either side of the graft-host junction from 4 to 12 weeks. A radio-lucent zone is usually evident between implant and callus, but in some instances radio-dense material is seen directly adjacent to the implant. At 24 weeks the graft-host junctions are so well consolidated that the location of the junction is generally not identifiable on the X-rays. The implant-bone junctions do not appear to consolidate, and the radiographic appearances do not confirm or deny the existence of a bond.

Careful dissection of the implants harvested to date has shown that none of the implants was bonded in place. This observation has also been made with implants which appeared to be closely coapted with calcified matter on the X-rays.

Mechanical tests of the bioglass-coated alumina implants retrieved at sacrifice at both 12 and 24 weeks show about a 10% reduction in strength compared to unimplanted control specimens. The data to date is too scant to be statistically significant.

Discussion

The implant materials used in this study have passed the *in vivo* proof test for bonding ability [4]. Thus the lack of bond formation is most likely due to other than material factors, since the 45S5 bioglass has been shown to bond to bone in several other animal species [5-7]. The most likely cause of non-union seems to be that the implants were free to move, since they were not rigidly fixed to the host bone. This motion must have ceased, however, after a few weeks when the implant became entrapped in the callus. This suggests quite strongly that the bonding process is a sequential process, and if the sequence is interrupted by motion or some other cause bonding will not occur.

Future Work

Histological studies of the tissues surrounding the fibular implants, and scanning electron microscope analyses of the surfaces of the unbonded implants, are currently being performed to establish further clues as to the reason for non-unions of these implants, as well as to identify the types of tissues surrounding the implants.

Harvesting of all implants will be completed by mid-December, and shortly after that all mechanical tests of retrieved implants and graft-host junctions will be completed. Analysis of the retrieved specimens for porosity, cumulative bone formation, and cumulative callus formation will begin within the next two weeks.

References

1. W. F. Enneking, H. Burchardt, J. J. Puhl, and G. Piotrowski, "Physical and Biologic Aspects of Repair in Dog Cortical Bone Transplants," J. Bone & Jt. Surg., 57-A:237-252, 1975.
2. D. C. Greenspan and L. L. Hench, "Chemical and Mechanical Behavior of Bioglass-Coated Alumina," J. Biomed. Mater. Res. Symp., No. 7, pp. 503-509, 1976.
3. P. Buscemi and L. L. Hench, "An Immersion Process for Coating Metal Implants with Bioglass," this report, pp. 55.
4. M. Walker, T. Carr, S. Gould and G. Piotrowski, "Materials Screening for Bonding Ability," this report, pp. 50.
5. G. Piotrowski, L. L. Hench, W. C. Allen, and G. Miller, "Mechanical Studies of the Bone-Bioglass Interfacial Bond," J. Biomed. Mater. Res. Symp., No. 6, pp. 47-61, 1975.
6. P. Griss, D. C. Greenspan, G. Heimke, B. Krempien, R. Buchinger, L. L. Hench, and G. Jentschura, "Evaluation of a Bioglass-Coated Al_2O_3 Total Hip Prosthesis in Sheep," J. Biomed. Mater. Res. Symp., No. 7, pp. 511-518, 1976.
7. G. J. Miller, D. C. Greenspan, G. Piotrowski, and L. L. Hench, "Mechanical Evaluation of Bone-Bioglass Bonding," presented at the 2nd Annual Meeting of the Society for Biomaterials, April 9-13, 1976, Philadelphia, PA.

F. Histological Studies of the Bone-Bioglass Interface--A Progress Report, M. S. Harrell, H. A. Paschall and L. L. Hench

A number of rats have been implanted with rat tibial chips, as described in previous sections of this report, for periods of up to one year. These specimens thus represent a complete time sequence, of much longer duration than heretofore studied. Most of these specimens have been harvested and sections for both light and transmission electron microscopy are being prepared.

One of the preliminary findings from this series involves the erosion of bioglass where it is in contact with the contents of the marrow cavity. Some necrotic tissue is in evidence, and erosion of the bioglass has taken place, at the one year time period. Some rats are currently implanted for longer in vivo tests, to ascertain whether this process is stable, i.e., self-limiting, or unstable.

Additional examinations of the bone-bioglass bond are being performed using the scanning transmission electron microscope, and a critical point drying technique for specimen preparation. This latter technique leads to sections of the interface which are not damaged in the drying process. The resulting undisturbed picture of the morphology of the interface, confirms the existence of a bulk bioglass: SiO_2 -rich layer: Ca-P rich film: bone transition zone.

A major paper, elucidating the time sequence of bone formation using a variety of microscopic techniques, is currently being prepared and should be completed within the next two months.

G. Clinical Biomechanics, G. Piotrowski.

Introduction

Tissues, implants, limbs, and bodies all obey certain basic laws which can be described by mathematical expressions of the relationships between forces and motions. Application of these descriptions of the real world are primarily within the purview of the physical scientist and the engineer. Thus, the training of these individuals equips them uniquely to contribute substantially to the analysis of retrieved implant devices to assess the causes for failure. The application of the concepts of mechanics to the medical field has been lumped under the heading "biomechanics;" I am not very comfortable with this term, since it implies that what I do in studying things in the body is basically different than what I do in studying the failure of a bearing cap of an internal combustion engine.

Now that I've alienated all of my friends who are "bioengineers," let me hasten to point out that in looking inside the body we are dealing with an irregular geometry, non-linear materials, ill defined loading patterns, and a few other factors which make analysis of the forces, displacements, stresses, and strains experienced by the implant very difficult. The principles are the same as propounded in basic engineering courses, but the mathematics can become almost nightmarish.

The Philosophy of Biomechanics Analysis.

The principles involved in "biomechanical analysis" of implants are easily outlined, as in Figure 1, but generally very difficult to implement. In the general case, one begins with a free-body analysis, isolating the object of interest from its environment, and identifying all interactions (forces, fluid flows, deflections, etc.) between the object and its environment. Force and moment equilibrium conditions are applied to establish relationships between known and unknown forces, and if we're lucky these will suffice to allow us to find the unknown forces. For statistically indeterminate cases, however, the equilibrium conditions are not sufficient to lead us to a complete description of the state of the object, and we must invoke the concept of compatibility of deformations. Finally, constitutive relations are introduced to relate loads and deformations. The resulting mathematical description of the object under study may be quite complex, but solutions of these equations will yield the desired data on loads and deformations experienced by the object.

In the above overview, it was tacitly assumed that the object is in static equilibrium, and that the forces were constant in both magnitude and orientation. These conditions are, however, not true for many significant cases, and ignoring these time variations of forces and velocities may lead to substantial errors. If the inertial forces are not insignificant, or if the force vectors vary with time, the above analysis must be applied repeatedly, and solutions for each instant of time must be obtained. Clearly this leads to lengthy computations.

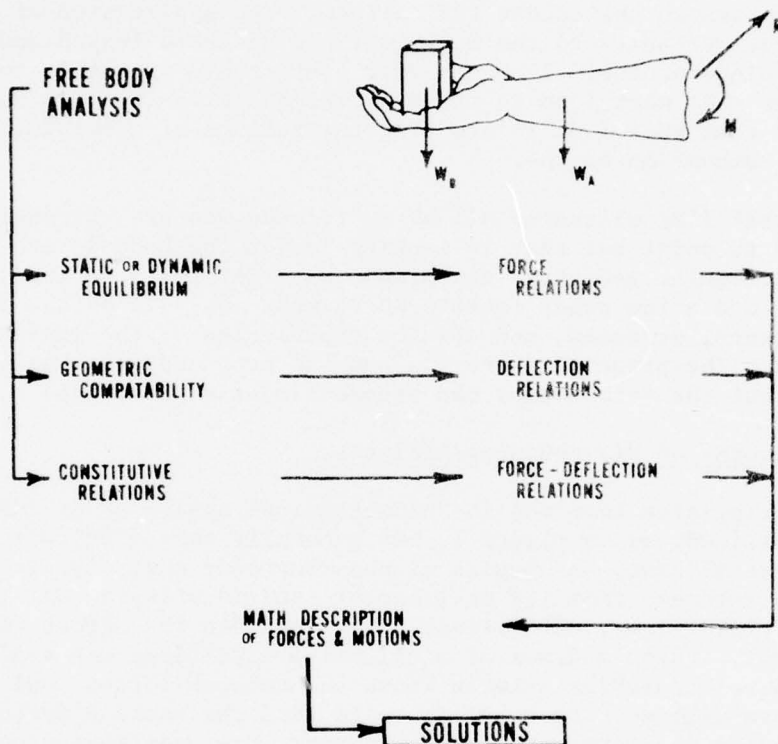


Fig. 1. All biomedical analysis approaches make use of equilibrium conditions, geometric compatibility, and/or constitutive relations to deal with the object of interest, as defined by the "free body," and to attain solutions to biomechanical problems.

Once the loads and/or deformations on the implant have been defined, material properties are involved to establish the stresses, or force intensities, at every point of interest in the device as suggested by Figure 2. Computing the stresses at selected points of interest, however, frequently implies calculating stresses everywhere in the object. It is at this point that the fields of materials science and mechanics merge, since both deformations and stresses are determined by the applied loading, the geometry of the device, and its material properties.

It is important at this point to differentiate formally between the terms "applied load" and "strength". The former term refers to the force conditions the device is subjected to, while the latter term describes how much load the device can sustain before bad things happen to it. The applied load is established through the procedure outlined above and differs for every analysis, while the strength depends on the properties of the material and geometry of the implant. One must also distinguish between various strengths, as defined by the various mechanical modes of failure so well described earlier by Dr. Williams.

I will present two case histories which illustrate how an analysis of the mechanics of the implant involved contributed to or even changed the conclusions regarding the cause of failure, and only briefly highlight some of the many varied and complex techniques used.

Case I.

A sixteen year old white male involved in an automobile accident sustained a fracture of the right femur in the vicinity of the junction of the proximal and middle thirds. The fracture was treated with a 9 mm cloverleaf intramedullary nail. About three weeks later, the youth experienced sharp severe pain in his right thigh while putting on his pants (standing up) and felt the nail bend. X-rays (Figure 3) confirmed the bend and a closed partial straightening was performed. The nail was bent again at 24 weeks post-op in a fall, removed, and replaced by a new 9 mm cloverleaf nail. The fracture proceeded to heal uneventfully, and the second nail was removed routinely 15 months after the original fracture.

A metallurgical study of the bent nail produced no evidence of surface defects or anomalous microstructure. X-ray spectrographic results indicated that the composition was "very likely" type 316 stainless steel. A yield strength of 470 MPa (68 kpsi) and a hardness of 25 HRC were measured and deemed to be reasonable. Thus, since no material defects or deficiencies were noted, a biomechanical design analysis was recommended to determine the loads.

In order to assess the loads at the fracture site during the critical maneuver of putting on one's pants, several motion picture sequences were made of a subject of similar weight and stature as the patient. One frame of the film, shown in Figure 4, which was judged to be the most critical, was traced onto a large sheet of paper. Anthropomorphic data published by Drillis et al [1] was used to locate and weigh the centers of mass

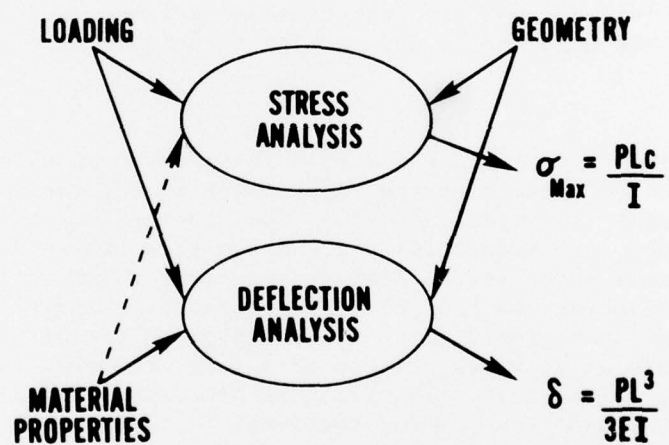
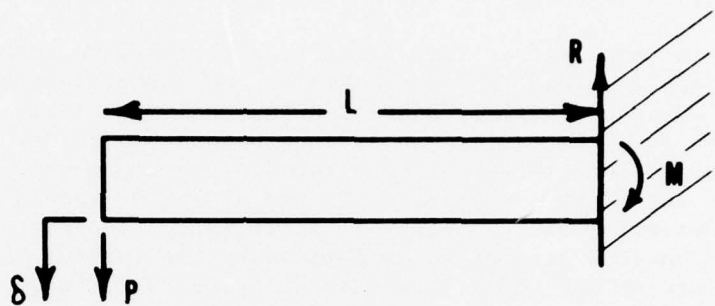


Fig. 2. The analysis of stresses and deflections requires that the loading, obtained as shown in Figure 1, and the material properties be combined with the description of the object's configuration.

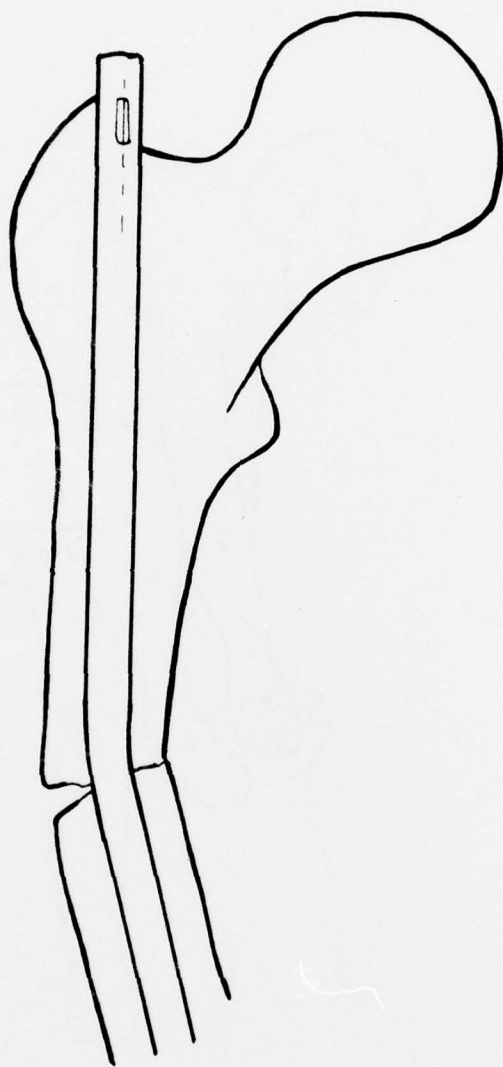


Fig. 3. This tracing of an X-ray shows the bend suffered by a 9 mm cloverleaf nail when the patient put on his pants while standing up at 3 weeks post-operatively.

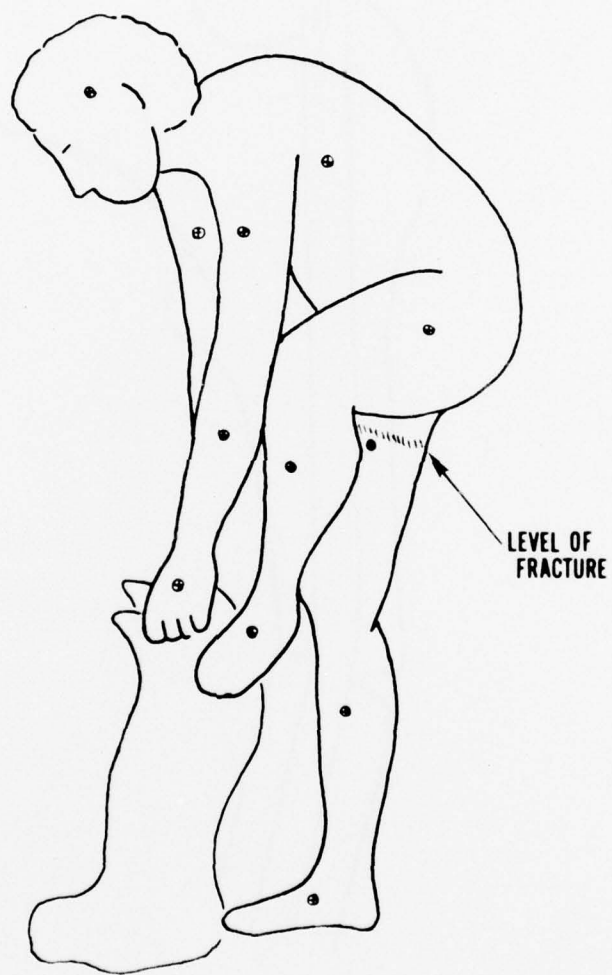


Fig. 4. Configuration of a subject filmed in the act of dressing himself. Note the position of the upper body is far in front of the fracture site.

of each of 15 body segments on the two views of the subject. The locations of the center of mass of the entire body, of the right lower extremity below the fracture site, and remainder of the body were then calculated. The maneuver was assumed to be quasistatic, and inertial forces were neglected. Since the center of mass of the entire body was found to be located directly above the right foot, which was the single support for the entire body, a reasonable amount of confidence in the appropriateness of the analysis was acquired.

A free body analysis of the body proximal to the fracture site showed that a net compressive load of 547 N (123 lbf) and a bending moment of 92.1 N·m (815 in lbf) had to be transmitted across the cross section of the thigh at the fracture site. Furthermore, this moment tended to bend the thigh in an antero-medial direction.

The compressive load is manifested in a compressive stress across the fracture site. This stress is quite tolerable and, in fact, thought by some to be essential for bone healing. The bending load, however, has two factors involved. A major portion of it is resisted by the bending of the nail itself, while the balance originates from the fact that the hamstrings act at some distance away from the center of the femur. These two components of the bending load at that cross section are difficult to separate rigorously. However, some very interesting comparisons may be made as depicted in Figure 5. The yield moment of a 9 mm cloverleaf nail, based on a yield strength of 690 MPa (100,000 psi) for cold worked stainless steel was calculated to be about 22.6 N·m (200 in. lb.) (at this point yielding just began at the points furthest away from the neutral axis). A solid "nail" of the same outer diameter would exhibit a yield moment of about 49.1 N·m (435 in. lb.). Both of these calculated values are well below the applied bending load.

Clearly, the hamstrings must, in fact, be tensed. Acting at a distance of about 75 mm, they would have to exert a force of about 925 N (210 lbf) to protect the nail. While these muscles can exert such forces quite readily, they would also act to flex the knee, which is bad since the knee is already slightly flexed. Thus, to keep the leg in the configuration required to support the body, the hamstrings and quadriceps must maintain a substantial force differential. However, the nail can only withstand a small portion of these forces exerted within the thigh. Furthermore, the body has little feedback information to tell it that the nail is getting bent. The nail is thus easily bent during this extremely strenuous behavior, and the implant "fails". One must conclude that the bending of the intra-medullary nail was a consequence of the large load applied through the patient's actions, and would not have been prevented by the use of a different nail design or different material.

Case II

A 61 year old white male had had generalized arthritis for many years. Persistent pain in his left knee led to an attempt to fuse the joint. A Hansen-Street nail was driven through the length of the femur and half the length of the tibia. The nail blocked motion, but some of the pain persisted. About three years post-operatively, the patient felt a sharp snap in his left knee when he stepped off a curb. Swelling and increased motion ensued.

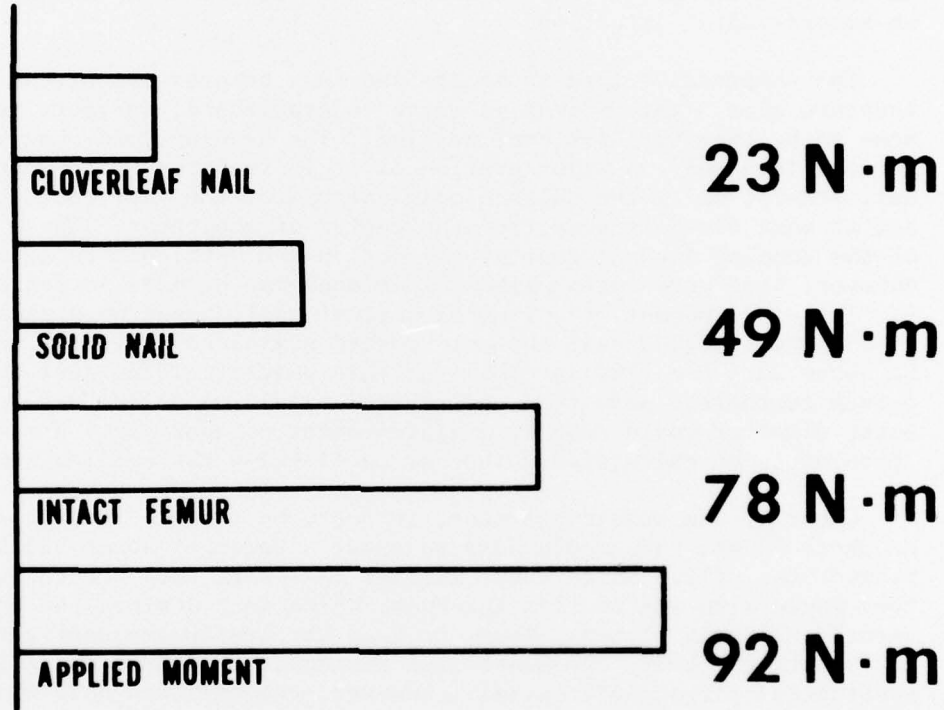


Fig. 5. Comparison of the strengths of the cloverleaf nail, a solid rod of stainless steel, an intact femur, and the bending moment applied to the thigh at the fracture site.

The intramedullary nail was seen on X-ray (Figure 6) to be fractured. Upon the removal of the implant the fracture surface presented an appearance characteristic of fatigue failure as depicted in Figure 7. The flat areas show where the fatigue cracks grew under the cyclic loading, leaving only the central ridge to snap off for the final failure. The gouge marks visible on the implant apparently were created during the removal of the implant. Unfortunately the marks obscure the question of whether any stress concentrators, due to either manufacturing defects or technical errors by the surgeon, were present prior to the fracture and acted to facilitate the failure.

As before, a free-body diagram of the implant, drawn in Figure 8, is illustrative of the type of load seen by the nail. The muscles of the leg continue reflexively to try to flex and extend the knee despite the presence of the nail. While the magnitude of the forces cannot be obtained without much work, the morphology of the loading on the nail can readily be established. The bending moment experienced by the nail in the vicinity of the knee can then readily be plotted in a qualitative fashion. The crucial feature of this moment diagram is that the bending moment is largest in the joint space between the femur and the tibia, and this moment is reasonably constant across that space. Closer examination of the implant, Figure 9, showed that another fatigue crack existed about 5 mm distal to the break in the anterior surface of the nail. A matching crack, although not as well developed, was found on the posterior side. The original surfaces of the implant are still visible in the vicinity of this crack, and no surface defects were evident under 40 X visual observation. A metallographic section through the incomplete cracks also revealed no abnormalities. Thus, the incomplete fatigue crack did not originate at an overt defect. Since both cracks occurred under identical conditions of loading (i.e. both cross sections were subjected to the same bending moment), one can safely conclude that formation of the failure crack was also not enhanced by any surface defects, and the nail was placed in a situation where it was overloaded in cyclic bending.

Without the consideration of the (bio) mechanics of the nail's failure, the integrity of the nail's surface would have remained in question. The nail itself was not defective, but its application for this situation was erroneous. Again, I would raise the question as to whether such missapplication could be avoided if the surgeon was provided with data outlining the mechanical characteristics of the nail.

Summary

The principles of mechanics, applied to a clinical situation, can be used to define or describe the forces and stresses acting on an implant. These data must be combined with the metallurgical analysis to describe, in a comprehensive fashion, what led to the failure of an implant. When only one or the other of the analyses is performed, incorrect conclusions may be readily drawn, leading to erroneous corrective actions or charges. Only when the expertise of both fields is applied to the retrieved implant, will a consistently correct assessment of its success or failure be made.



Fig. 6. X-ray of a Hansen-Street nail, intended to fuse the knee, which failed abruptly about three years after implantation.

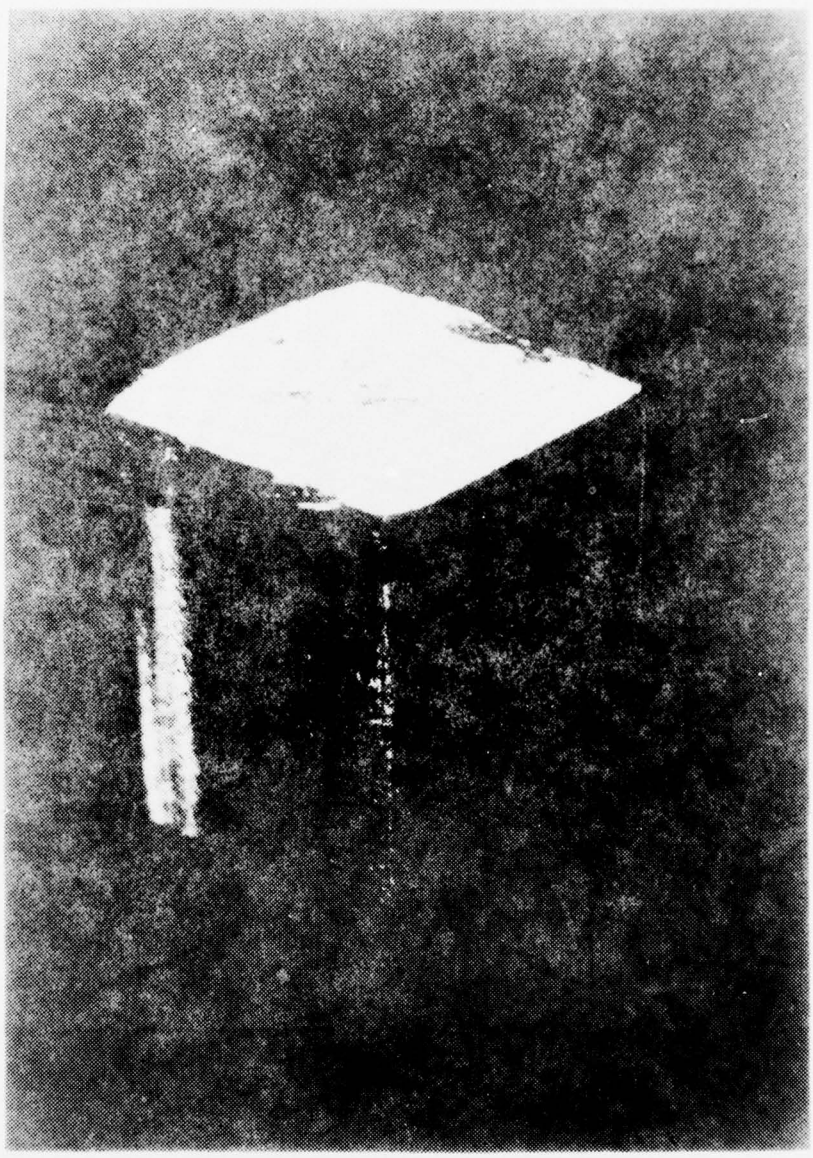


Fig. 7. The fracture surface of the implant shown in Figure 6 presents an appearance typical of a fatigue failure in reversed bending. The central ridge running horizontally across the diamond-shaped cross section was the last part to fail.

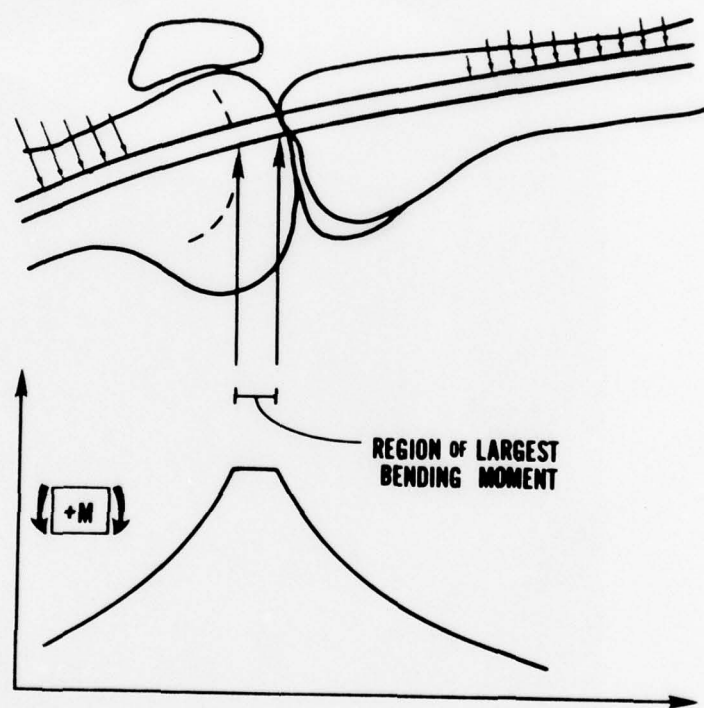


Fig. 8. Freebody analysis of the implant shown in Figure 6 prior to its failure shows that the bending moment experienced by the nail is quite constant across the joint space.



Fig. 9. Another view of the fracture surface of the nail shows another fatigue crack about 5 mm distal to the fracture surface.

References

1. Drillis, R., R. Contini and M. Bluestein (1964), Body Segment Parameters, Artificial Limbs, 8 (no. 1): 329-351.

DISTRIBUTION LIST

Commanding General U. S. Army Medical Research and Development Command ATTN: MEDDH-SI Washington, D. C. 20314	4
Defense Documentation Center ATTN: DDCIR Cameron Station Alexandria, Virginia 22314	12
Commanding Officer U. S. Army Combat Development Command Medical Service Agency Brooke Army Medical Center Fort Sam Houston, Texas 78231	1
National Institute of Dental Research Dental Materials Science Bethesda, Maryland 20014	1
NASA Materials Science Division Washington, D. C. 20546	1
Army Research Office - Durham Metallurgy and Ceramics Division Durham, North Carolina	1
National Institute of Health Division of Orthopaedics Bethesda, Maryland	1
Defense Ceramic Information Center Battelle Memorial Institute 505 King Avenue Columbus, Ohio 43201	1
National Institute of Health National Institute of General Medical Sciences Bethesda, Maryland 20014	1
Colonel Simon Civjan, DC Chief, Division of Dental Materials U. S. Army Institute of Dental Research Washington, D. C. 20012	1

SECURITY CLASSIFICATION OF THIS PAGE (When Data Entered)

REPORT DOCUMENTATION PAGE		READ INSTRUCTIONS BEFORE COMPLETING FORM															
1. REPORT NUMBER 7	2. GOVT ACCESSION NO. ⑦	3. RECIPIENT'S CATALOG NUMBER Rept. no. 7															
4. TITLE (and Subtitle) AN INVESTIGATION OF BONDING MECHANISMS AT THE INTERFACE OF A PROSTHETIC MATERIAL.		5. TYPE OF REPORT & PERIOD COVERED (Annual) Report Oct. 1, 1975-Sept. 30, 1976															
6. AUTHOR(s) L. L. Hench, William C. Allen, Homer A. Paschall and George Piotrowski 10		7. PERFORMING ORG. REPORT NUMBER 1 Oct 75 - 30 Sep 76 15															
8. CONTRACT OR GRANT NUMBER(s) DAMD 17-76-C-6033		9. PERFORMING ORGANIZATION NAME AND ADDRESS University of Florida Department of Materials Science and Engineering Gainesville, Florida 32611															
10. PROGRAM ELEMENT, PROJECT, TASK AREA & WORK UNIT NUMBERS		11. CONTROLLING OFFICE NAME AND ADDRESS U. S. Army Medical Research and Development Command Washington, D. C. 20314															
12. REPORT DATE October 1976		13. NUMBER OF PAGES 80															
14. MONITORING AGENCY NAME & ADDRESS (if different from Controlling Office) 12/81P.		15. SECURITY CLASS. (of this report)															
		15a. DECLASSIFICATION/DOWNGRADING SCHEDULE															
16. DISTRIBUTION STATEMENT (of this Report) Approved for public release; distribution unlimited																	
17. DISTRIBUTION STATEMENT (of the abstract entered in Block 20, if different from Report)																	
18. SUPPLEMENTARY NOTES																	
19. KEY WORDS (Continue on reverse side if necessary and identify by block number) <table style="width: 100%; border-collapse: collapse;"> <tr> <td style="width: 33%;">Bioceramics</td> <td style="width: 33%;">Transmission electron microscopy</td> <td style="width: 33%;">Bone growth</td> </tr> <tr> <td>Glass</td> <td>Scanning electron microscopy</td> <td>Glass-ceramics</td> </tr> <tr> <td>Orthopaedics</td> <td>Auger electron spectroscopy</td> <td>Microstructure</td> </tr> <tr> <td>Hydroxyapatite</td> <td>Infrared reflection spectroscopy</td> <td>Solubility</td> </tr> <tr> <td>Collagen</td> <td>Bone</td> <td>(continued)</td> </tr> </table>			Bioceramics	Transmission electron microscopy	Bone growth	Glass	Scanning electron microscopy	Glass-ceramics	Orthopaedics	Auger electron spectroscopy	Microstructure	Hydroxyapatite	Infrared reflection spectroscopy	Solubility	Collagen	Bone	(continued)
Bioceramics	Transmission electron microscopy	Bone growth															
Glass	Scanning electron microscopy	Glass-ceramics															
Orthopaedics	Auger electron spectroscopy	Microstructure															
Hydroxyapatite	Infrared reflection spectroscopy	Solubility															
Collagen	Bone	(continued)															
20. ABSTRACT (Continue on reverse side if necessary and identify by block number) <p>The surface chemical behavior of bioglass containing soda-calcia-silica and variable percentages of phosphorous has been investigated. Many techniques: infrared reflection spectroscopy, ion solution analysis, scanning electron microscopy, energy dispersive x-ray analysis, x-ray diffraction, Auger electron spectroscopy, ion beam milling, have been used to understand a simulated physiologic environment. Surface ion concentration profiles determined with Auger spectroscopy and ion beam milling detail the structural (continued)</p>																	

408174

JRC

19. (continued)

Selective leaching	Implant	Fatigue strength
H	Surfaces	Paired bones
P	Biomechanics	Composite
Nucleation	Cancellous bone	Bone plate
Crystallization	Flame spray	
Interfacial bonding	Femur	
Mechanical strength	Segmental bone replacement	
Proteins	Rats	
Epitaxy	Monkeys	
Crystals	Strain measurement	
Kinetics	Computer calculations	
Histology	Torsional strength	
Stress analysis	Stainless steel	

20. (continued)

alterations produced by aqueous attack and in vivo exposure. Organic constituents C and N, not present in the bioglass, are found incorporated into the reactive surface of bioglass for distances up to 1800 Å. A mechanism is postulated which explains the sequence of events leading to the formation of the multiple-layer corrosion structures in vivo. Stable interfacial fixation results when bioglasses are implanted in bone, provided good initial fixation is obtained. Based upon the in vivo observations, a theory is proposed that an ideal implant material must have a dynamic surface chemistry that induces histological changes at the implant surface which would normally occur if the implant were not present. An in vivo proof test of bonding ability has been developed and used to show that this bond forms consistently. The same test is presently being used to determine the range of bioglass compositions capable of forming a bond to bone. A new technique of coating stainless steel with bioglass has been used to produce implants which form bonds with bone as readily as bulk bioglass. This material system will lead to implants whose mechanical properties, i.e., strength and rigidity, are governed by the metal substrate, and whose surface characteristics and ability to bond to bone stems from their bioglass coatings.